Technical University of Crete
School of Electrical and Computer Engineering

Diploma Thesis

Modeling of trigeneration system in Buildings

Dimitrios A. Manelas

Examining Committee

Professor Kanellos Fotios (Supervisor)

Professor Stavrakakis Georgios

Associate Professor Gyftakis Konstantinos

Chania, Crete, August 2023

Acknowledgements

In a nutshell, I would like to genuinely thank my supervisor, Professor Kanellos Fotios, for providing me with the opportunity to deal with such an interesting and topical thesis. It was his experience and guidance that helped me to successfully complete my diploma work. Furthermore, I would like to express my appreciation to the Ph.D. student Kyriakou Dimitra, for her interest and invaluable assistance.

Last but not least, I staunchly express my deepest gratitude and gratefulness to my family for giving me the opportunity to study in the department of "Electrical and Computer Engineering" at the Technical University of Crete and for supporting me in every step I made.

Dimitrios A. Manelas

Abstract

It is a fact that the energy demand for cooling, heating and electricity has been steadily increasing over the years. In particular, rapid development in the industrial, commercial and residential sectors have contributed to the growth in energy consumption. This constantly-increasing energy demand has led to a significant reduction in fuel reserves. Continuing at this rate would result in a depletion of fuel sources. Additionally, this irrational extensive use has also an impact on greenhouse gas and pollutant emissions. Consequently, it is an imperative need to adopt more efficient and environmentally friendly ways of using energy sources. In an attempt to overcome this upcoming problem, trigeneration may be a solution.

In this framework, an integrated trigeneration system for residential use is proposed and examined under different operating scenarios. To this end, a comprehensive investigation of the trigeneration concept is presented. Trigeneration or CCHP (Combined Cooling, Heating, Power) is the term referring to systems that can simultaneously produce and provide cooling, heating and electricity from a single source. In conventional systems, such as those currently in use, most of the energy provided by the fuel (approximately 60 to 70 percent) is converted to heat and dissipated into the environment. A portion of the heat released as a by-product of power generation is recovered and used for heating and cooling applications through the trigeneration system. Considering building's thermal loads and other operational parameters, a proper selection of the prime mover, refrigeration system and other components assembling the CCHP system is achieved. Hence, Stirling engine and absorption chiller have been selected for the proposed system. An extensive analysis of these components is performed. Building thermal loads modelling is also carried out. In this way, realistic data representing typical building loads were extracted and used to verify the proper operation of the system. PSO algorithm was used with the purpose of minimizing the operating cost of the grid-connected CCHP system. This algorithm determines system's operational behavior and finds the optimum operation profile, considering several constraints such as the grid electricity price and the demand of the building loads. All the developed models comprising the CCHP system are verified through the simulation of realistic case studies. Hence, results are extracted and discussed for different operating scenarios over a 24-hour period.

Key words: Trigeneration system, CCHP system, Fuel efficiency, Prime mover, Refrigeration system , PSO algorithm

Περίληψη

Είναι γεγονός ότι οι ενεργειακές απαιτήσεις για ψύξη, θέρμανση και ηλεκτρισμό έχουν αυξηθεί τα τελευταία χρόνια. Συγκεκριμένα, η ραγδαία ανάπτυξη στον βιομηχανικό, εμπορικό και οικιακό τομέα συμβάλλει στην αύξηση της κατανάλωσης ενέργειας. Αυτή η ολοένα και περισσότερο αυξανόμενη ζήτηση της ενέργειας, έχει οδηγήσει στην μείωση των ενεργειακών αποθεμάτων. Εμμένοντας σε αυτόν τον ρυθμό, αποτέλεσμα θα είναι η εξάντληση των πηγών καυσίμων. Επιπλέον, αυτή η εκτεταμένη χρήση έχει αντίκτυπο στις εκπομπές αερίων ρύπων που εντείνουν το φαινόμενο του θερμοκηπίου. Συνεπώς, είναι επιτακτική ανάγκη η υιοθέτηση πιο αποδοτικών και φιλικών προς το περιβάλλον μεθόδων χρήσης των πηγών ενέργειας. Σε μια προσπάθεια να ξεπεραστεί το επερχόμενο πρόβλημα, η τριπαραγωγή πιθανόν να αποτελεί λύση.

Σε αυτό το πλαίσιο, ένα ολοκληρωμένο σύστημα τριπαραγωγής για χρήση σε οικεία προτείνεται και εξετάζεται υπό διαφορετικά σενάρια λειτουργίας. Για αυτό τον σκοπό, παρουσιάζεται μια περιεκτική διερεύνηση της έννοιας της τριπαραγωγής. Ο όρος τριπαραγωγή (ή αλλίως συνδυασμένη ψύξη, θέρμανση και ηλεκτρισμός) αναφέρεται σε συστήματα τα οποία μπορούν ταυτόχρονα να παράγουν και να παρέχουν ψύξη, θέρμανση και ηλεκτρισμό μόνο από μια πηγή ενέργειας. Στα συμβατικά συστήματα, όπως αυτά που χρησιμοποιούνται προς το παρόν, το μεγαλύτερο μέρος της ενέργειας που παρέχεται από το καύσιμο (περίπου το 60 με 70 τοις εκατό) μετατρέπεται σε θερμότητα και διαχέεται στο περιβάλλον. Ένα μέρος της θερμότητας που απελευθερώνεται ως υποπροϊόν της ηλεκτροπαραγωγής ανακτάται και χρησιμοποιείται για εφαρμογές θέρμανσης και ψύξης μέσω του συστήματος τριπαραγωγής. Λαμβάνοντας υπόψιν τα θερμικά φορτία του κτιρίου και άλλες λειτουργικές παραμέτρους, επιτυγχάνεται η κατάλληλη επιλογή της κινητήριας μηχανής, του συστήματος ψύξης και άλλων εξαρτημάτων που συνθέτουν το σύστημα τριπαραγωγής. Ως εκ τούτου, ο κινητήρας Stirling και ο ψύκτης απορρόφησης επιλέγονται για το προτεινόμενο σύστημα. Πραγματοποιείται εκτεταμένη ανάλυση για τα επιλεγμένα εξαρτήματα. Πραγματοποιείται επίσης μοντελοποίηση των θερμικών φορτίων του κτιρίου. Με αυτόν τον τρόπο, εξήχθησαν ρεαλιστικά δεδομένα που αντιπροσωπεύουν τυπικά φορτία οικείας και χρησιμοποιήθηκαν για την επαλήθευση της ορθής λειτουργίας του συστήματος. Έγινε χρήση του αλγόριθμου PSO με σκοπό την ελαχιστοποίηση του κόστους λειτουργίας του συνδεδεμένου στο δίκτυο συστήματος τριπαραγωγής. Ο συγκεκριμένος αλγόριθμος καθορίζει το βελτιστο προφίλ λειτουργίας, λαμβάνοντας υπόψη διάφορους περιορισμούς, όπως είναι η τιμή της ηλεκτρικής ενέργειας του δικτύου και οι απαιτήσεις των φορτίων του κτιρίου. Όλα τα μοντέλα που αναπτύχθηκαν και συνθέτουν το σύστημα τριπαραγωγής επαληθεύονται με ρεαλιστικές προσομοιώσεις. Έτσι, εξάγονται και σχολιάζονται αποτελέσματα για διαφορετικά σενάρια λειτουργίας διάρκειας 24 ωρών.

Contents

Figures

Nomenclature

Abbreviations

CCHP	Combined Cooling Heating Power
COP	Coefficient of Performance
EP	Electricity Price
FEL	Following Electric Load
FHL	Following Hybrid Load
FL	Flexibility
FP	Fuel Price
FTL	Following Thermal Load
HHV	Heating value of fuel
m.u.	monetary unit
LiBr	Lithium Bromide
PSO	Particle Swarm Optimization
SoC	State of Charge

Engine Parameters

C_p	Helium specific heat at constant pressure $(J/kg\ k)$
C_v	Helium specific heat at constant volume $(J/kg\ k)$
fr	Frequency (Hz)
hw_c	Hot water coefficient
gA_i	Mass flow in working space i (kg/s)
M	Total mass of working gas (kg)
M_{FF}	Mass flow rate of fuel (kg/h)
m_i	Instantaneous mass in working space i (kg)
n_g	Electric generator efficiency
p	Engine pressure (Pa)
P	Power output (W)
Q_{ach}	Actual heat input (W)
Q_{ack}	Actual dissipated heat (W)
Q_i	Heat transfer through working space i (W)
R	Helium gas constant $(J/kg\ k)$
T_i	Temperature in working space i $(Kelvin)$
uf	Usage factor
V_i	Volume in working space i (cc)
W	Work output (J)
γ	Specific heat ratio $(C_p \cdot C_v)$
θ	Crank angle (deg)

Absorption Chiller

Eff	Efficiency
h_i	Enthalpy in chiller's working space i (kJ/kg)
m_i	Mass flow of solution pair i (kg/s)
Q_i	Heat transfer through chiller's component i (W)
x	Solution concentration (%)

Hot water storage tank

SW	Stored water
T_{ref}	Reference temperature of hot water
T_{urb}	Incoming water temperature to be heated

Thermal Loads model

a_w	External wall absorbance coefficient
C_z	Specific heat capacity
$FL_z^{\uparrow}$	Upper flexibility of zth thermal zone
$FL_z^{\downarrow}$	Lower flexibility of zth thermal zone
F_wall , F_win	Surface area of wall/window
$I_{T,z}$	Total solar radiation
p_z	Density of zth thermal zone
$\dot{Q}_{ex,wall,z}$	External wall heat exchange (kW)
$\dot{Q}_{in,wall,z}$	Internal wall heat exchange (kW)
$\dot{Q}_{in,z}$	Internal heat gains (kW)
$\dot{Q}_{sg,z}$	Solar radiation through the windows (kW)
$\dot{Q}_{sw,z}$	Heat gains of ex. wall's solar radiation (kW)
$\dot{Q}_{win,z}$	Heat transfer across the windows (kW)
R_{se}	Heat resistance of the external surface
SC	The shading coefficient of the window
U_{wall} , U_{win}	Factor of the heat exchange of the external wall/window
V_z	Volume of the air of the zth thermal zone
τ_{win}	Window glass transmission coefficient

Energy System Modeling

P_{grid}	Active power supplied from the grid
P_{bat}	Active power of the battery
n_{ch}	Charging efficiency coefficient
n_{disch}	Discharging efficiency coefficient

Sets and indices

bat	Battery
c	Compression chamber
ck	Compression-cooler space interface
e	Expansion chamber
el	Electric
h	Heater
he	Heater-expansion space interface
k	Cooler
kr	Cooler-regenerator space interface
mech	Mechanical
r	Regenerator
rh	Regenerator-heater space interface
wh	Heater wall
wk	Cooler wall
abs	Absorber
con	Condenser
ev	Evaporator
g	Generator
hx	Heat exchanger
$\mathcal{E}$	External wall set
ex	External
in	Internal
nz	Neighboring thermal zones
y	yth external wall/window index
z	zth thermal zone index
hw	Hot water

Chapter 1

1. Introduction

1.1 General

Over the past years, it has been observed that the energy demand for cooling, heating and electricity has been steadily increasing. More specifically, developments in the industrial sector, services and households contributed to the growth of energy consumption in heating and cooling. Energy consumption is influenced by many social and economic factors and drivers. It is a fact that the ever-increasing consumption of fuel has led to a noticeable reduction in the fuel reserves. As a result, fuel sources are becoming more and more scarce. Continuing at this rate would result in a depletion of fuel sources. It also has a significant impact on greenhouse gas and pollutant emissions from the combustion of fossil fuels for power generation. Therefore, in order to solve the upcoming problem, more efficient and environmentally friendly ways of using fuel sources are being investigated. In an attempt to get around this impending impasse, trigeneration may possibly be a solution.

1.2 Trigeneration

Trigeneration or CCHP systems are capable of producing and cover cooling, heating and electricity demands simultaneously from a single source. In conventional systems, most of the energy provided by the fuel (approximately 60 to 70 percent) is converted to heat and dissipated into the environment. A portion of the heat released as a byproduct of power generation is recovered for cooling and heating applications rather than being rejected to the atmosphere. Wasted thermal energy is typically used for space heating or hot water and space cooling. Thus, no further fuel consumption is required for these applications. A higher level of efficiency is observed when compared with conventional separate heat and power systems. CCHP systems have been used at times in industrial, commercial and residential buildings. Nevertheless, it is easy to understand that the size and operation of such a system is proportional to the building type in which it is used and the operation strategy. The operation strategy is extremely important as it directly affects thermal performance and operational cost of the system. Scholars have conducted several researches on the operating strategies, with the most common being the Following electric load (FEL) and Following thermal load (FTL) [1]. Other strategies are usually consisting of a synthesis of the above such as Following hybrid electric-thermal load (FHL) [2].

A typical configuration of a CCHP system consists of a gas prime mover to convert thermal energy of fuel into mechanical energy, a power generation unit to provide electricity and a heat recovery system in order to regather the thermal energy released during engine operation. Thermally activated units then provide heating and cooling using the recovered thermal energy. Each of the trigeneration components is appropriately selected based on the type of load being used. More specifically, engines such as internal combustion engines, turbines and external

combustion engines can be used as system's prime mover. Chilled water can be provided by either absorption or adsorption refrigeration system which are thermally activated units. A variety of heat exchangers such as heating coils or finned tubes, can be used along with a thermal storage tank to store hot water. For the operation of the overall system, proper synthesis and cooperation of the above subcomponents is essential.

Trigeneration is one of the most widespread distributed generation system. Distributed generation term generally refers to electricity production near the consumption. In this manner, it appears to have some of the advantages provided in such systems. First and foremost, can operate both in islanded mode, supplying consumer's local demand, or grid-connected mode supplying energy to the electric power system. The power flow is bi-directional, which means the system can both supply power to the grid and be supplied by the grid improving grid reliability and providing a higher level of robustness. In this way, a possible surplus of energy is supplied to the grid and is not wasted, which would otherwise be the case. This creates opportunities for power trading in a competitive environment and contributes to the recovery of a percentage of system operating costs. In addition, because most of the power is generated and consumed in the same area, transmission losses are limited, while energy costs are reduced by eliminating reliance on expensive main grid peak tariffs. Another advantage of distributed generation CCHP systems is that they can also be easily integrated into microgrids [3].

In addition to the benefits that trigeneration offers as a distributed generation system, there are a number of other advantages that make it an enticing choice. Therefore, compared to conventional systems, the worth noting advantages that CCHP system take precedence are as follows:

- Fuel efficiency: The use of existing waste heat for cooling and heating applications improves the utilization of the fuel source. No additional fuel is required.

- Environmental impact: Higher value of overall efficiency and lower amounts of fuel consumption contribute to reduction of pollutant emissions.

- Fuel flexibility: They are capable of using a wide variety of fuel sources, such as fossil fuels, organic fuels, or even fuels derived from renewable energy sources.

- Flexibility: Can be used as both a primary and a backup source of power, ensuring the reliability of the power plant.

- Independence: Trigeneration systems provide a reliable, independent power source that eliminates grid fees and potential power interruptions, especially in remote locations.

1.3 Thesis Overview

The purpose of this thesis is to propose a trigeneration system for building applications and present realistic results of its operation. To this end, a comprehensive review of the trigeneration concept is presented. In this way, a proper selection of the prime mover, refrigeration system and

other components assembling the CCHP system is achieved. This selection is proportional to the load of the building being served, user input parameters, and other system specifications that are discussed below. An extensive analysis of the selected components comprising the proposed system has been performed. In order to minimize the operating cost of the grid-connected CCHP system, the PSO algorithm was used. Several constraints were considered such as grid electricity price and building's loads at that time. Realistic data representing typical building loads were used as case study variables for system operation simulation and results extraction.

Chapter 2 outlines the advantages of specific prime movers and refrigeration systems that provide incentives for their selection for the proposed CCHP system. It then provides an in-depth analysis of these components.

Chapter 3 examines a number of user and system constraints under which the trigeneration system should operate. There is also a brief review of the PSO algorithm used for minimizing the system operating cost.

Chapter 4 presents the case study in which the CCHP system is being studied. It specifies the constraint values presented in the previous section and gives the corresponding results.

Chapter 5 presents general conclusions derived from the obtained results. It also includes suggestions for future continuity and extension of the present work.

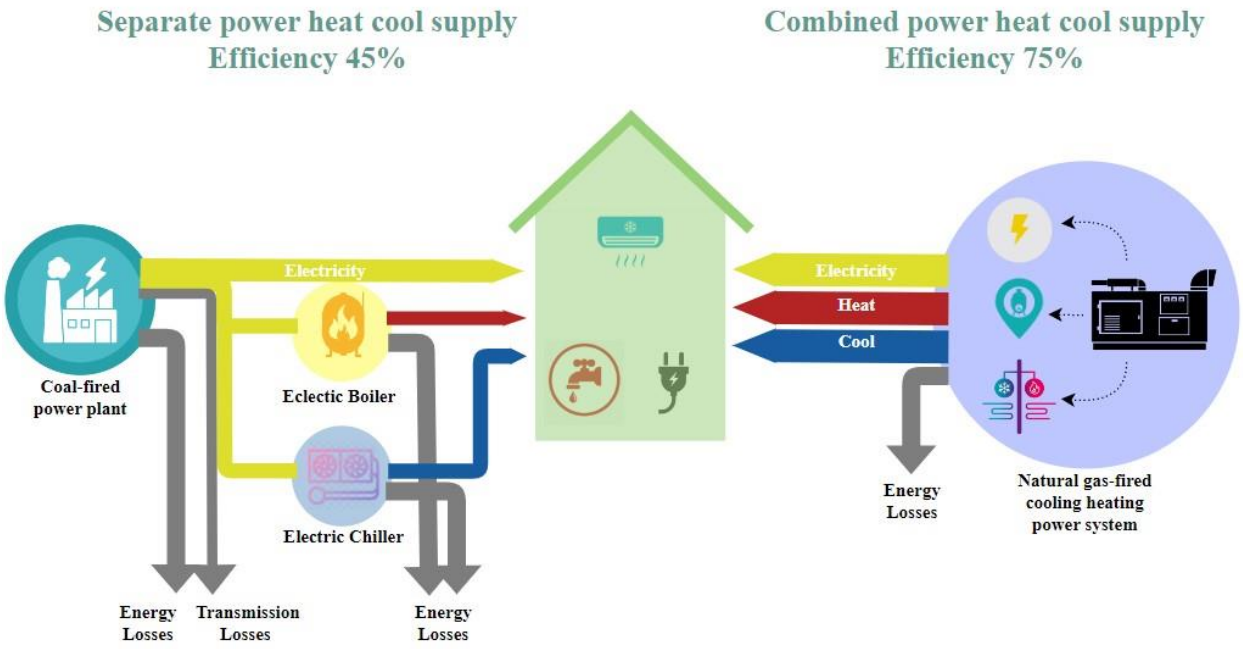

Fig. 1 CCHP - Conventional systems

Chapter 2

2. Models

2.1 CCHP Subsystems Selection

Conventional systems efficiency is usually less than 40%. That means that more than 60% of the input heating value is lost to the environment. The use of low efficiency systems for building's energy needs has a significant impact on fuel consumption and emissions. Consequently, research for more efficient systems is under investigation. Compared to conventional systems, CCHP systems appear to be about 30-40% more efficient and have therefore been on the top of the preference list. With the aim of reducing energy consumption and emissions to the environment, a CCHP system is proposed to cover the energy needs of the building. This system is capable of simultaneously generating the building's electricity, cooling and heating needs without any additional fuel supply. The system consists of a prime mover engine that combusts fuel to drive the shaft of the generator. This provides electrical power to the building. The thermal energy dissipated by the prime mover is used to activate the CCHP subsystems to cool and heat. The type and configuration of the prime mover and associated subsystems will depend on the electricity, cooling and heating demand profile of the building.

Prime mover

The prime mover is the main component of the CCHP and should be carefully selected to meet several system requirements. A variety of engine types can be selected for use as a prime mover. However, there are some major advantages of the Stirling engine that make this type of engine an appropriate selection as a prime mover: [4]

The fuel combusts separately from the engine. This allows a variety of fuels to be used in combination with an appropriate combustion system. In addition, non-conventional energy sources, such as organic fuels, could be used as a heat source, which contributes to the reduction of pollutant emissions.

Hydrogen and helium are the most commonly used working fluids due to their high heat transfer rate and high specific heat capacity. By using these working fluids, high thermal efficiency of the Stirling engine is achieved.

Because the engine's expansion and compression chambers are sealed, the working fluid does not come into contact with atmospheric air and other corrosive substances that could damage the engine. Therefore, low maintenance is required.

Rhombic drive mechanism used in the proposed Stirling engine consists of two similar symmetrically arranged gears. As a result, the movement of the piston and the displacer is carried out in such a way that low-noise operation is achieved.

During the engine cooling process, a usable amount of waste heat is dissipated from the engine. In addition, the thermal energy that was not converted into mechanical work can be recovered as well. All of the recovered thermal energy can be utilized for thermally activated processes.

Cooling system

The cooling system should be easily integrated with CCHP systems, and in particular with the engine that will be used in the proposed system. Therefore, a proper selection should consider the above mentioned as well as the thermal load requirements of the building. In the proposed CCHP system, a single effect LiBr-water absorption chiller is selected for cooling purposes as more relevant. Some of the key features of the absorption chiller that were the basis for this selection are: [13]

Absorption chillers are thermally activated cooling systems. This allows the engine's waste heat to be used directly without any conversion that would cause additional energy loss.

A single effect chiller, such as the one used in the proposed system, operates with heat input generator temperatures ranging from 80 to 120°C. This is in line with the cooler temperature of the engine, which is operating at a similar temperature, so waste heat can be utilized.

Since water is used as refrigerant for the LiBr-water solution pair, absorption chiller must operate at temperatures above 0°C. Although this does not pose a problem as long as the absorption chiller is used for air conditioning purposes.

There are no moving parts in the absorption chiller. As a result, maintenance costs are very low. Additionally, when considering it as a part of a CCHP system due to its technology, the overall lifecycle costs are low.

Considering the aforementioned, Stirling engine and absorption chiller were selected as the prime mover and cooling system, respectively, of the proposed CCHP system. Fuel is supplied to provide the energy needed to run the Stirling engine. Natural gas has been used as fuel in the proposed system. The mechanical power output of the Stirling engine is converted to electrical by means of a generator. During engine operation, heat is dissipated from cooler component so as to keep its temperature low. Therefore, since the prime mover is an external combustion engine, a remarkable amount of thermal energy is dissipated to the environment during power generation. The above waste thermal energy which would otherwise be lost to the environment, is now recovered to power the absorption chiller and heat water without the use of additional fuel. A thermal load model is proposed in order to evaluate buildings' thermal loads depending on several parameters. This will help to obtain results for the CCHP system that are representative of the real world. [6]

The following subsections provide a comprehensive review of each component of the CCHP system. The structure of the components, principles of operation, characteristics and other various assumptions are presented. The engine analysis is performed based on non-ideal adiabatic model, which was conducted using a developed numerical code. Thermal and frictional

losses are considered. Analysis of absorption chiller is based on mass and energy conservation. The waste thermal energy is separated for cooling and heating applications depending on the demand at a given time and other constraints that will be discussed in the next section.

2.2 Stirling engine

2.2.1 About Stirling engine

The prime mover that is selected for the CCHP system is an external combustion engine, known as "Stirling engine". Despite the fact that this kind of engine was invented before other types, due to rapid development of internal combustion engine, Stirling engine was severely hampered for years. Nowadays, where the threat of global drain of energy sources and the steep increase of emissions have been an issue of a great importance, more efficient ways to cover the energy demands are investigated.

A Stirling engine is a heat engine that aim to transfer a mass of working gas in a way that is compressed at the cold area and expanded at the hot area in order to produce motion of the piston. Inductive heat exchange happens through the engine wall. This type of engine consists of 5 components which are the compression, expansion chambers and heater, regenerator, cooler heat exchangers the use of which will be discussed further below. Consider a cylinder with two opposed pistons and a regenerator which is interpolated in between. The area enclosed by the regenerator and the right piston is expansion volume. Similarly, compression volume is consisted of the area between regenerator and left piston. Heater adds heat in order to maintain temperature of expansion chamber high. On the other hand, cooler absorbs heat so that compression chamber temperature maintains low. [5]

The ideal thermodynamic Stirling cycle consists of two processes of isothermal compression and expansion, and two processes of isochoric heat addition and rejection in the working fluid. Figure 2 shows the sequence of the four processes that are mentioned above.

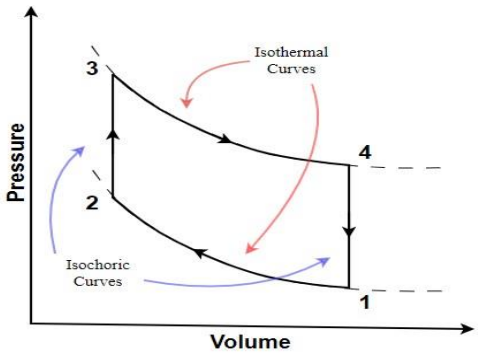

Fig. 2a PV diagram for SE

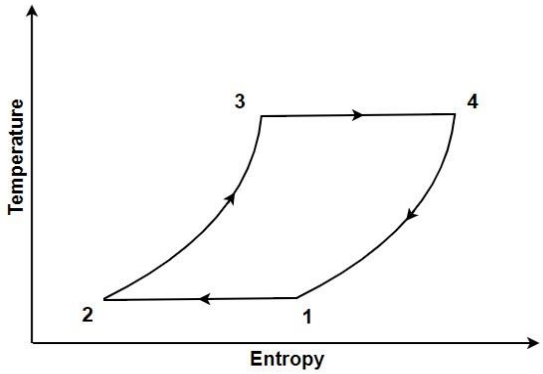

Fig.2b TS diagram for SE

In order to examine the Stirling cycle we assume compression piston at outer dead point and expansion piston at inner dead point. Hence, total mass of working fluid contained in compression space. Temperature and pressure of the cycle are minimum represented by point 1 on PV diagram.

Stirling Cycle

Isothermal compression process $1 \rightarrow 2$, compression piston moves towards regenerator while the expansion piston remains stationary due to phase angle. Hence, volume is reduced and pressure of working fluid increases from P_1 to P_2. Temperature is maintained constant due to heat flow from cooler heat exchanger to the surrounding. Work done on the working fluid equals the amount of rejected heat during process.

Constant volume regenerative transfer process $2 \rightarrow 3$, expansion piston starts moving away from regenerator. In that way, both pistons move at the same time so that volume between pistons remains constant. Working fluid is transferred from compression to expansion space via regenerator. Hence, heat is added through regenerator and temperature increased from T_{min} to T_{max}. The gradual increase in working fluid temperature while passing through regenerator causes increase in pressure. Consequently, there is an increase in fluid's entropy and internal energy. Volume remains constant during this process so no work is done.

Isothermal expansion process $3 \rightarrow 4$, compression piston remains stationary at inner dead point besides regenerator while expansion piston continues to move towards outer dead point. Fluid pressure decreases as expansion volume increases. Although, temperature remains constant at T_{max} by adding heat from external source via heater heat exchanger. Work done on piston equals in magnitude the heat supplied from heat source. There is an increase in entropy of working fluid while the internal energy remains constant.

Constant volume regenerative transfer process $4 \rightarrow 1$, both pistons move simultaneously so as to transfer working fluid from expansion to compression space at constant volume and complete thermodynamic cycle. Hot working fluid is transferred through regenerator which absorbs heat and reduces fluid's temperature to T_{min}. Because of heat rejection, there is a decrease in internal energy and entropy of working fluid. No work is done during this process.

Stirling thermodynamic cycle as described above is highly idealized because of the requirements that implies. More specifically, first assumption of isothermal working and heat exchange imply that the heat exchangers are required to be perfectly effective and in order to achieve this, infinite rate of heat transfer is required between cylinder wall and working fluid. However, second assumption stipulates no heat transmission between engine walls and working fluid in order to prevent heat losses. Consequently, in actual engine operation, neither of the assumptions is fulfilled.

Engine configuration

With respect to their mechanical arrangement, Stirling engines are classified into three main groups of configuration, i.e. alpha, beta and gamma. Each configuration follows the same thermodynamic cycle as described previously with different mechanical design characteristics.

Alpha configuration engines consist of 2 power pistons, known as hot and cold piston. They are located in 2 separate cylinders connected in series by a heater, regenerator and cooler. Working fluid is transferred between hot and cold cylinder where the expansion and compression occurs, respectively. Both pistons are attached at the same crankshaft and contribute to produce work.

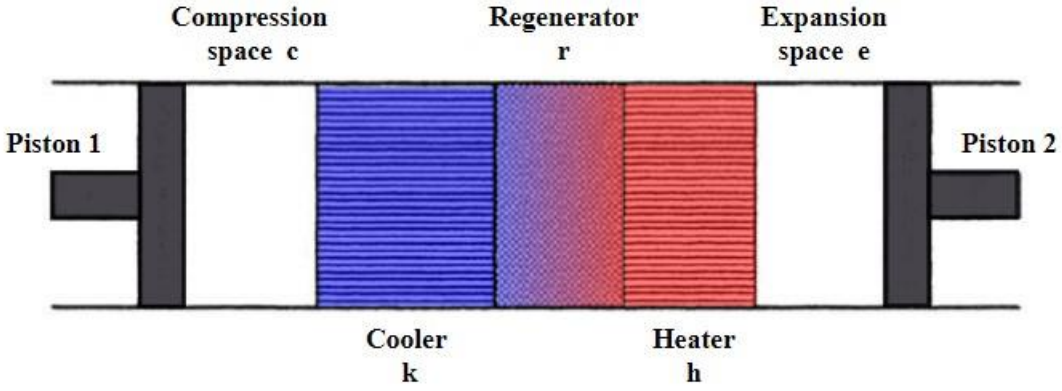

Fig. 3 Alpha-type configuration of SE

Beta configuration engines use a displacer-piston arrangement in the same cylinder, as shown in Figure 4. Power piston is located at cold space of the cylinder, compresses and expands the working fluid when it is at the cold or hot space, respectively. Working fluid is transferred from expansion to compression space and vice versa by means of displacer. Piston and displacer are connected at the same crankshaft using different linkages so as to provide required phase angle.

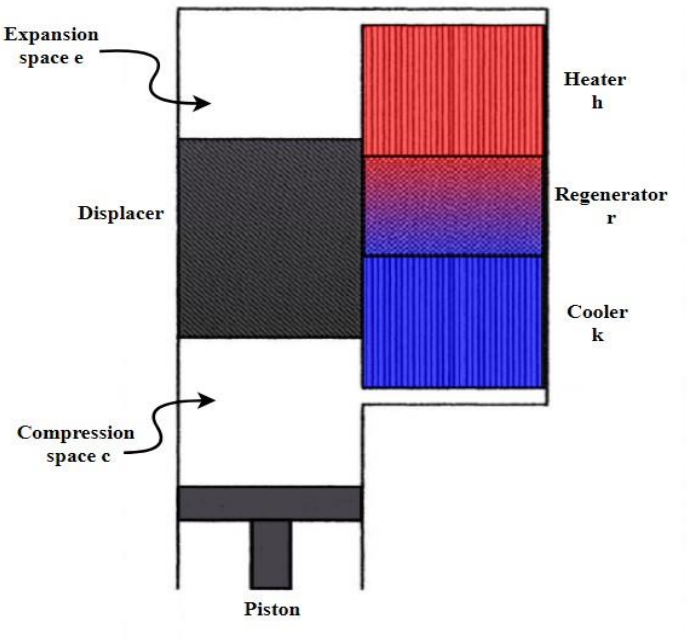

Fig. 4 Beta-type configuration of SE

Gamma configuration engines use separated cylinders for the displacer-piston arrangement. Compression space splits between 2 cylinders with an interconnecting transfer port. Displacer moves working fluid between hot and cold space of the cylinder through heater, regenerator and cooler series. There is another gamma-configuration which consists of double acting piston arrangement and theoretically has higher possible mechanical efficiency. Work occurs by means of piston motion.

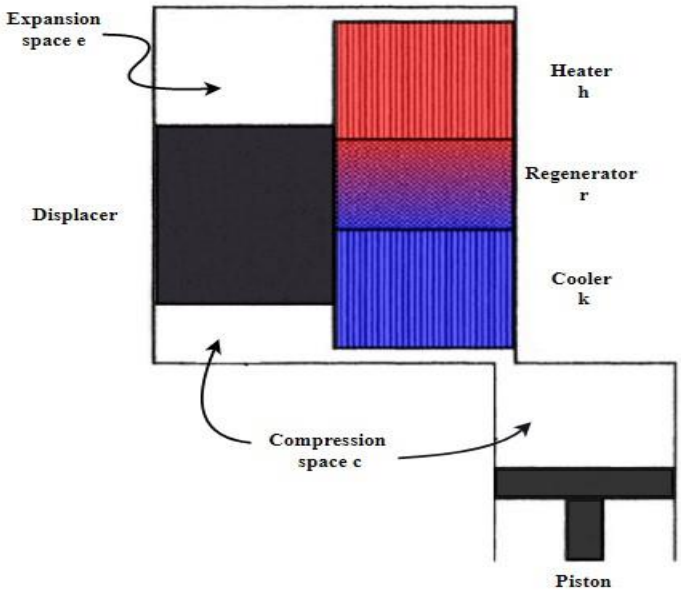

Fig. 5 Gamma-type configuration of SE

2.2.2 Isothermal analysis

The first attempt to analyze the operation of the Stirling cycle was published by Schmidt in 1871. This analysis lays the groundwork for other researches that published during the following years. The analysis, known as the Isothermal analysis, targets to determine the relations for the produced work of the engine and the heat transfer during the cycle. The main assumption of this analysis is that temperature of the working fluid remains at a specific high (Th) value at expansion and heater components as well as in compression and cooler components remains at specific low (Tk) temperature. Hypothesis of isothermal working spaces and exchangers implies there is no heat loss. Thus, heat exchangers of the engine are ideal. Also, volume variation of compression and expansion spaces assumed to be sinusoidal. [7]

Other assumptions that are required to be taken into account in order to model the isothermal analysis, are the following:

1. Mass of the working fluid remain constant, there is no gas leakage.
2. Working fluid considered as ideal gas.
3. Frequency of Stirling cycle is constant.

4. Thermal equilibrium has been occurred.
5. Kinetic and dynamic gas energy are ignored.

The objective of Schmidt analysis is to establish a comprehensive mathematical approach of Stirling cycle. Thus, considering the aforementioned assumption of mass conservation and ideal gas law formula, following relations are carried out:

$$M = m_c + m_k + m_r + m_h + m_e \tag{1}$$

Using ideal gas law equation:

$$m = \frac{p*V}{R*T} \tag{2}$$

Replacing ideal gas equation to (1):

$$M = \frac{p*\left(\frac{V_c}{T_c}+\frac{V_k}{T_k}+\frac{V_r}{T_r}+\frac{V_h}{T_h}+\frac{V_e}{T_e}\right)}{R} \tag{3}$$

Ideal regenerator heat follows linear profile and is computed by mean logarithmic difference temperature of heater and cooler exchangers:

$$T_r = \frac{T_h - T_k}{ln\left(\frac{T_h}{T_k}\right)} \tag{4}$$

Solving for pressure at (3) equation:

$$p = M * R * \left(\frac{V_c}{T_k} + \frac{V_k}{T_k} + \frac{V_r * ln\left(\frac{T_h}{T_k}\right)}{T_h - T_k} + \frac{V_h}{T_h} + \frac{V_e}{T_h}\right)^{-1} \tag{5}$$

The above equation gives pressure variation of working gas as a function of working spaces volume variation.

Produced work occurs by the volume variation of working spaces during operation. Hence, over a complete cycle of the engine the total work equals the algebraic sum of compression and expansion spaces work.

$$W = W_c + W_e = \oint p \cdot dV_c + \oint p \cdot dV_e = \oint p \cdot \left(\frac{dV_c}{d\Theta} + \frac{dV_e}{d\Theta}\right) d\Theta \tag{6}$$

where Θ is stroke angle.

Heat transfer from working gas to the environment and vice versa occurs at low and high temperature chambers, respectively. In order to investigate the amount of heat exchange at heater and cooler of the engine, energy equation of working gas is used. A generalized cell of working space which may be either a working space or a heat exchanger is shown in the figure below. Enthalpy enters the cell via gas flow $gA_i\ (kg/s)$ and temperature $T_i\ (K)$ and exits through gas flow $gA_o\ (kg/s)$ and temperature $T_o\ (K)$. Where mass flow gA represents mass flux $m\ (kg/m^2 s)$ multiplied by free flow area $A\ (m^2)$. Indices i and o denote to inlet and outlet valves.

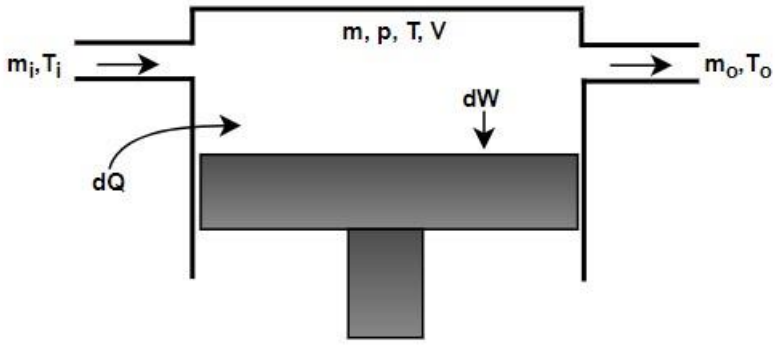

Fig. 6 schematic representation of a generalized cell

Energy equation in a generalized cell is:

$$[Rate\ of\ heat\ tranfer\ into\ cell] + [Rate\ of\ incoming\ net\ enthalpy] = [Rate\ of\ work\ produced] + [Rate\ of\ internal\ energy\ increase\ in\ cell]$$

Mathematically the above expression becomes:

$$DQ + \left(C_p T_i g A_i - C_p T_o g A_o\right) = DW + C_v D(mT) \tag{7}$$

Where $D \equiv \frac{d}{dt}$ and C_p, C_v are specific heat capacity of the working gas at constant pressure and volume, respectively. Equation (7) is the standard form of energy equation for the case that there is no steady flow, where kinetic and dynamic energy can be bypassed.

With consideration of isothermal assumption of constant temperature for working spaces as well as for heat exchangers, we have that $T_i = T_o = T$.

Hence, energy equation becomes:

$$DQ = -C_p T(gA_o - gA_i) + C_v T Dm + DW \tag{8}$$

Because of mass conservation, the mass accumulation rate in the cell equals the difference between mass flow, i.e. $D_m = gA_i - gA_o$. Along with the relation that governs ideal gasses which is $R = C_p - C_v$, equation (8) becomes:

$$DQ = DW - RTDm \tag{9}$$

Total amount of heat transferred to the working gas during every cycle is given by a cyclic integration of energy equation:

$$Q = \oint DQ = \oint DW - R \cdot T \oint Dm \tag{10}$$

Having a thermal equilibrium means that cyclic variation of working gas mass is zero for every cell component. Thus, applying energy equation for working spaces and heat exchangers of the engine, following results are taken.

For working spaces: $$Q_c = W_c \, , Q_e = W_e \tag{11}$$

For heat exchangers: $$Q_k = 0 \, , Q_h = 0 \tag{12}$$

The obtained results show that needed heat is exchanged via working spaces and heat exchangers doesn't contribute at any heat transfer. As a consequence, cooler and heater components of the engine can be bypassed. This outcome due to constant temperature assumption for working spaces. Although, the above statement will be turned over later on adiabatic analysis.

2.2.3 Ideal adiabatic analysis

As the isothermal model impose, temperatures of the expansion and compression chambers have constant value as the engine operates. This led to the paradoxical situation that neither heater nor cooler exchangers contribute any heat transfer, thus making them redundant. Needed net heat transfer happens across the boundaries of the isothermal working space. Although, working space design for expansion and compression processes doesn't meet the needs of practical and effective heat exchange. Consequently, in operation of real machines compression and expansion chambers tend to be adiabatic rather than isothermal. So, at every operation cycle of the engine heat is supplied through heat exchangers.

A major advantage at isothermal analysis was that relations which model the engine are easily integrated. However, taking into consideration that expansion and compression temperature is varying during the engine cycle, integration isn't feasible. As a result, arithmetic method is implemented to model the adiabatic analysis. This type of model approaches in a better way the operation of the Stirling engine in real world. It was Finkelstein who made the first complete attempt to analyze the adiabatic model in 1960.

Non-isothermal analysis assumed that only a part of the heat from working chambers is transferred as a function of a heat transfer coefficient, hence there is a temperature variation during the cycle. As a result, between the components of the engine there is a temperature discontinuity due to the temperature variation at working spaces. Finkelstein in order to overtake this, he suggested a method called "the conditional temperature". In that way, while the working gas flew in the engine components, the instant temperature has the same value as the temperature of the space that it came from. Other design parameters were further added in the adiabatic model by Walker and Kahn in order to study the analysis. Therefore, the effects of temperature ratio between hot and cold end exchangers, phase angle, swept and dead volume ratio were examined.

Adiabatic model provides an extension of isothermal analysis. It intends to analyze Stirling cycle in terms of non-isothermal working spaces. Assumptions mentioned in isothermal analysis such as mass and pressure conservation, are still valid. Hence, the sum of all individual cell masses equals total mass of the working gas in the engine. Work is produced due to the volume variations at working spaces Vc and Ve during engine cycle. The amount of heat exchange from heat source to the working fluid is symbolized as Qh. Similarly, the amount of dissipated heat from working fluid to the environment is indicated as Qk.

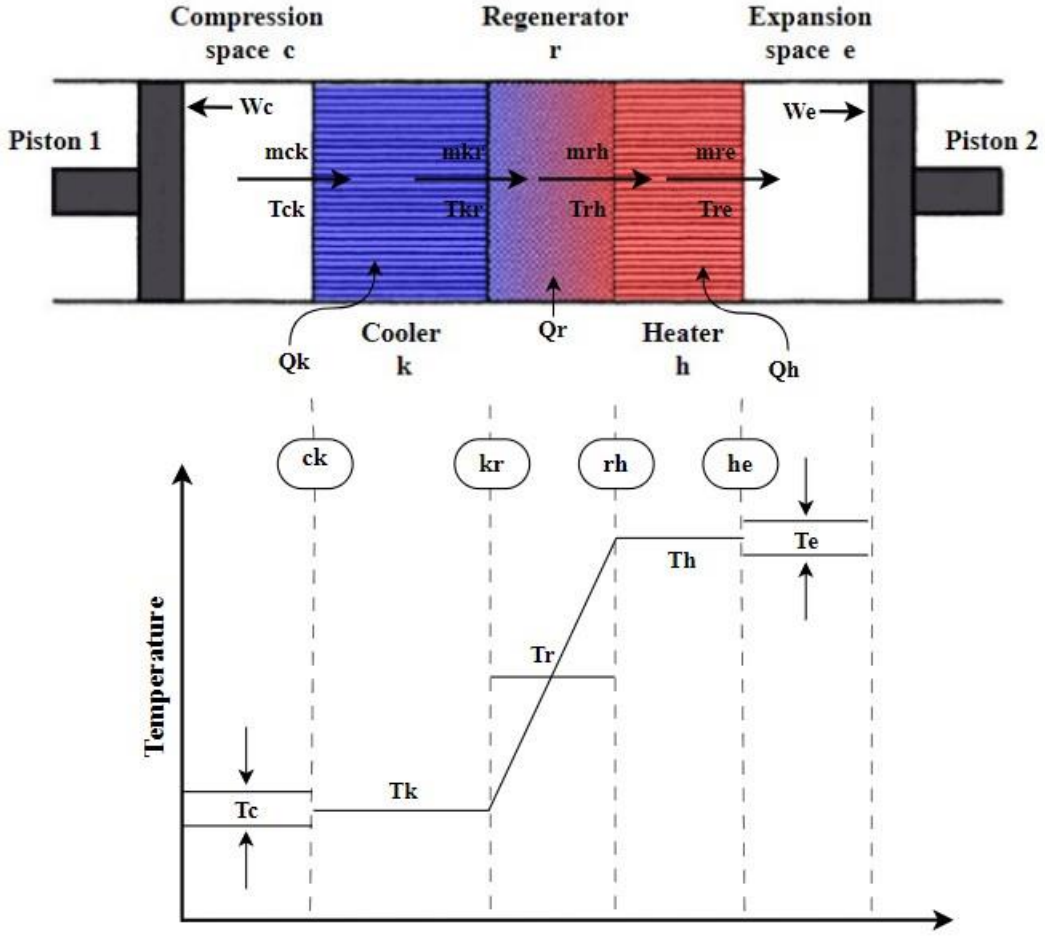

Fig. 7 Ideal adiabatic model and temperature distribution

Relations that describe the ideal adiabatic analysis, terminology and hypotheses that characterize the model are presented below. In this way, the engine behavior is determined under conditions that vary over cycle time. Moreover, an extensive investigation between adiabatic working spaces and engine performance is made. As mentioned at isothermal analysis, Stirling engine is a device which operates on a closed regenerative thermodynamic cycle with cyclic compression and expansion of the working fluid at different temperatures levels. The engine is divided into 5

components in sequence and each cell is examined individually. Interactions between each cell are also being studied.

Heater space temperature T_h which is controlled from engine's combustion system is maintained in isothermal condition. In a similar manner, cooler space temperature T_k is held at a constant low value from the engine cooling system. Heat exchangers are assumed to be ideal just as isothermal analysis. According to this approach, there are no regenerator losses to the environment. Consequently, regenerator as well as working fluid temperature located in that space have the same temperature follow linear profile and is computed by mean logarithmic difference temperature of heater and cooler exchangers.

$$T_r = \frac{T_h - T_k}{\ln\left(\frac{T_h}{T_k}\right)} \tag{13}$$

There are 4 separated areas through which engine's components come into contact. In further detail, (ck) notation will be used for the area connects compression space (c) and cooler exchanger (k). Hence, mass flow of working fluid referenced to this area will be symbolized as gA_{ck}. Conforming to the same rationale, notations (kr), (rh), (he) will be used for reference to cooler (k) and regenerator (r), regenerator (r) and heater (h), heater (h) and expansion space (e) connections, respectively. These notations are used in order to specify the engine area that each relation of adiabatic model is referred to. Mass flow direction from compression to expansion space has arbitrarily defined as positive route. Negative value means that reverse flow is observed.

Temperature of the above connecting areas are defined by "conditional temperature" method. Thus, T_{ck} and T_{he} temperatures vary during cycle and are directly proportional to mass flow of working fluid.

$$if\ gA_{ck} > 0 \quad then \quad T_{ck} = T_c \quad else \quad T_{ck} = T_k \tag{14}$$

$$if\ gA_{he} > 0 \quad then \quad T_{he} = T_h \quad else \quad T_{he} = T_e \tag{15}$$

Since the compression and expansion spaces tend to be adiabatic, the temperature of each space varies as the engine operates in accordance with the ideal gas law.

Expansion space temperature: $$T_e = \frac{p \cdot V_e}{R \cdot m_e} \tag{16}$$

Compression space temperature: $$T_c = \frac{p \cdot V_c}{R \cdot m_c} \tag{17}$$

Ideal adiabatic model relations, keeping up with isothermal analysis, are based on energy equation of working gas and formula of ideal gas law. In a generalized cell, energy equation is given by: [8], [9]

$$DQ + \left(C_p \cdot T_i \cdot gA_i - C_p \cdot T_o \cdot gA_o\right) = DW + D(m \cdot T) \tag{18}$$

Equation of state for ideal gasses is given by $PV = mRT$ and $C_p - C_v = R$.

Where $C_p = \frac{R \cdot \gamma}{\gamma - 1}$ and $C_v = \frac{R}{\gamma - 1}$.

Equation of state is converted to the form below by taking logarithm and differentiating as follows:

$$\frac{Dp}{p} + \frac{DV}{V} = \frac{Dm}{m} + \frac{DT}{RT} \tag{19}$$

As mentioned above, assumption for mass conservation of working gas remains valid.

$$M = m_c + m_k + m_r + m_h + m_e \tag{20}$$

Differentiating equation (20):

$$Dm_c + Dm_k + Dm_r + Dm_h + Dm_e = 0 \tag{21}$$

As long as heat exchangers volume and temperature remain constant during operation of the engine, equation of state for these components is transformed as follows:

$$\frac{Dp}{p} = \frac{Dm}{m} \tag{22}$$

Equation (21) applying equation (22) for every heat exchanger of the engine becomes:

$$Dm_c + Dp \cdot \left(\frac{m_k}{p} + \frac{m_r}{p} + \frac{m_h}{p}\right) + Dm_e = 0 \tag{23}$$

Then, substituting equation of state:

$$Dm_c + \frac{Dp}{R} \cdot \left(\frac{V_k}{T_k} + \frac{V_r}{T_r} + \frac{V_h}{T_h}\right) + Dm_e = 0 \tag{24}$$

In order to replace Dm_c and Dm_e terms, we apply energy equation for both working spaces where there is no heat input. Thus, for the compression space is:

$$DQc - C_p \cdot T_{ck} \cdot gA_{ck} = DWc + C_v \cdot D(m_c \cdot T_c) \tag{25}$$

Since working spaces tend to be adiabatic and heat transfer happens across the boundaries of heat exchangers of the engine, $DQc = 0$. As long as there is no gas leakage, rate of gas accumulation Dm_c equals mass inflow $-gA_{ck}$. Additionally, work done by compression space is computed as a function of volume variation, $DWc = p \cdot DVc$.

Considering the above observations combined with equation of state and associated ideal gas relations, equation (25) is reduced to:

$$Dm_c = \frac{\left(p \cdot DV_c + V_c \cdot \frac{Dp}{\gamma}\right)}{R \cdot T_{ck}} \tag{26}$$

Following the same path for the expansion space:

$$Dm_e = \frac{\left(p \cdot DV_e + V_e \cdot \frac{Dp}{\gamma}\right)}{R \cdot T_{he}} \tag{27}$$

Eventually, equation (23) replacing rates of gas accumulation Dm_c and Dm_e is transformed as follows:

$$Dp = \frac{-\gamma \cdot p \cdot \left(\frac{DV_c}{T_{ck}} + \frac{DV_e}{T_{he}}\right)}{\frac{V_c}{T_c} + \gamma \cdot \left(\frac{V_k}{T_k} + \frac{V_r}{T_r} + \frac{V_h}{T_h}\right) + \frac{V_e}{T_{he}}} \tag{28}$$

Once p and m_c variables are evaluated, other variables of the engine can be computed through the use of equation of state and equation of mass conservation. Volume variations Vc, Ve of working spaces and their derivatives DVc, DVe are available while all other parameters are constant. Tubes temperatures T_{ck} and T_{he} via of which components of the engine come into contact, are proportional to gas flow during engine operation and are specified from (14) and (15) statements. In order to evaluate the mass flow as well as specify the flow direction, continuity equation is utilized:

$$Dm = gA_i - gA_o \tag{29}$$

Hence, applying it for every cell component separately gives:

For compression space: $$gA_{ck} = -Dm_c \tag{30}$$

For cooler exchanger: $$gA_{kr} = gA_{ck} - Dm_k \tag{31}$$

For regenerator exchanger: $$gA_{rh} = gA_{kr} - Dm_r \tag{32}$$

For heater exchanger: $$gA_{he} = gA_{rh} - Dm_h \tag{33}$$

Furthermore, the mass accumulation at each heat exchanger component during the cycle time is evaluated by means of the ideal gas law.

For cooler exchanger: $$m_k = \frac{p \cdot V_k}{R \cdot T_k} \tag{34}$$

For regenerator exchanger: $$m_r = \frac{p \cdot V_r}{R \cdot T_r} \tag{35}$$

For heater exchanger: $$m_h = \frac{p \cdot V_h}{R \cdot T_h} \tag{36}$$

Algebraic sum of compression and expansion spaces, where there is volume variation as engine operates, gives the total work done per cycle:

$$DW = p \cdot DV_c + p \cdot DV_e \tag{37}$$

In order to evaluate the amount of heat transfer at each heat exchanger using equation of state and ideal gas relations, the following form of energy equation is obtained.

$$DQ + \left(C_p \cdot T_i \cdot gA_i - C_p \cdot T_o \cdot gA_o\right) = \frac{1}{R}\left(C_p \cdot p \cdot DV + C_v \cdot V \cdot Dp\right) \tag{38}$$

Heat exchangers volume during engine operation remain constant, as a result $p \cdot DV = 0$. In this regard we apply the aforementioned equation for every heat exchanger individually.

Cooler: $$DQ_k = V_k \cdot Dp \cdot \frac{C_v}{R} - C_p \cdot (T_{ck} \cdot gA_{ck} - T_{kr} \cdot gA_{kr}) \tag{39}$$

Regenerator: $$DQ_r = V_r \cdot Dp \cdot \frac{C_v}{R} - C_p \cdot (T_{kr} \cdot gA_{kr} - T_{rh} \cdot gA_{rh}) \tag{40}$$

Heater: $$DQ_h = V_h \cdot Dp \cdot \frac{C_v}{R} - C_p \cdot (T_{rh} \cdot gA_{rh} - T_{he} \cdot gA_{he}) \tag{41}$$

Since heater and cooler have been characterized as isothermal and regenerator tend to be ideal, it is noted that interface temperatures $T_{kr} = T_k$ and $T_{rh} = T_h$.

2.2.4 Working fluid selection

Working fluid that is contained in the expansion and compression chambers has a significant role of the engine performance. Although, when the first engines appear, air has been used as the main working fluid due to availability. Pressurized air has also been used so as to improve the efficiency. Nevertheless, other fluids were investigating for a better system performance. There are several fluid thermodynamic properties in order to reduce as much as possible thermal and frictional losses of the Stirling cycle, the most noteworthy are the following: [5]

1. High thermal conductivity.
2. High specific heat capacity.
3. Low viscosity.
4. Low density.

Martini, whose research is concentrated to select the most efficient working fluid, has also added another requirement. High capability of heat transfer of working fluid is the last property Martini added for better system performance. Heat transfer coefficient is defined as thermal conductivity of the fluid divided by the need of heat transfer and it is known as “capability factor”. [7]

$$Capability\ factor = \frac{Thermal\ conductivity}{(specific\ heat\ capacity)\cdot(density)}$$

Fluid properties range according to pressure and temperature that engine operates. In the table presented below, several fluids are compared using above equation at the same pressure and temperature equals 5Mpa and 800 K, respectively.

Working Fluid	*Heat Transfer*	*Capability factor*
Air	1.0	1.0
Helium	1.42	0.83
Hydrogen	3.42	0.68
Water	1.95	0.39
Sodium Potassium melt (Nak)	32.62	1.32

Table 1

From the table results, Nak eutectic seems to be the best selection compare to the others fluids. Although, knowing the course of Stirling engine it is noticed that (H_2) hydrogen and helium (He) are the main selection of researchers for working fluid. This dominant use of these fluids isn't justified from the table results. Nevertheless, main characteristics of both fluids make them a proper selection.

Hydrogen properties:

- Large thermal conductivity.
- Low viscosity.
- Low specific heat capacity at constant volume.

Helium properties:

- Low specific heat capacity at constant volume, lower than hydrogen.
- Thermal conductivity as good as that of hydrogen.
- Viscosity value twice that of hydrogen.

2.2.5 Heat exchangers

Heat exchangers add or reject heat from the working fluid of the engine, for that reason are of a great importance for Stirling engine performance. There are 3 heat exchangers in order to adjust and control the temperature of the working fluid in the engine. Heater transfers heat from an external source into the working fluid contained in the expansion chamber of the engine. On the other hand, cooler absorbs heat from the working fluid in the compression chamber. The

regenerator periodically accepts and rejects heat from working fluid and it is located between heater and cooler. [5], [7]

Heater:

Heater exchanger is a demanding component of the engine to design because it is affected by many engine specifications. The heater of the Stirling engine comes into contact with combustion system which is the heat source. Heat is transferred from heat source to walls and tubes of the heat exchanger by means of inductive heating. The outer tube surface usually experiences a high temperature, low pressure steady flow environment due to controlled operation of the combustion system. The inner tube surface experiences a high temperature, high pressure unsteady flow of working fluid due to non-isothermal chambers. It is of a great importance that produced heat from combustion system is distributed evenly so as to improve heater performance. Metals with high thermal conductivity are selected for heater design so a good heat transfer coefficient takes place with a small temperature difference at heat source. As the heater temperature rises, conductive working fluid absorbs heat and expands. For the reasons described above, heat exchanger design is selected as a function of the parameters by which is affected.

Cooler:

This engine component keeps the temperature of the working fluid in compression chamber at a desirable low temperature. The majority of Stirling engines are air or water cooled just like other type of engines, such as internal combustion. It is worth remembering that the absolute temperature between hot and cold end is directly proportional to engine efficiency. As a consequence, it is necessary to have coolant temperature at minimum possible value. Coolant fluid must be appropriately selected in order to serve two processes. The first one is maintaining low temperature constant despite hot end temperature changes. Secondly, the heat dissipated from engine cooler will be utilized for cogeneration, so a high heat transfer rate fluid with low thermal losses must be obtained.

Regenerator:

The purpose of using a regenerator is storing a part of heat supplied by heat source. Regenerator acts as a thermal sponge. More specifically, as the engine operates, working fluid temperature is converted from high to low value and vice versa. Regenerator absorbs heat during isochoric process $(4 \rightarrow 1)$ where the flow is from expansion to compression chamber at maximum temperature and returns it back in isochoric process $(2 \rightarrow 3)$ where the flow is from compression to expansion chamber at minimum temperature. Supposing an ideal regenerator, maximum and minimum temperatures of the process presented above would have constant values during engine operation. Ideal regeneration is possible only if heat transfer coefficient and area of heat transfer are infinite or operation is carried out infinitely slow. As a result, ideal regeneration isn't feasible. Efficiency depends on parameters such as thermal conductivity and length of regenerator. Other parameters that affect regenerator efficiency is that compression and expansion temperature,

pressure and flow of working fluid as discussed in adiabatic analysis is periodically changed. In this manner, it is easily understood that ideal regeneration isn't feasible.

In Figure 8, a main form of regenerator's temperature fluctuation is presented on account of Stirling cycle. Section (a) through (b) is related to hot flow period from expansion to compression chamber. On the other hand, section (b) to (c) represents cold flow period where the flow of working fluid is reversed. As it observed, fluid temperature is shifting from point A to point B when the heated fluid begins to flow through the regenerator. Curve B-C depicts the fluid temperature during heat flow period. Regenerator temperature follows the same curvature X-Y but has lower values since it stores certain amount of the provided heat. By the time flow rate changes, cold fluid supplied and fluid temperature reduced as shown in curve D-A. Regenerator exchanges the heat stored during heat flow period, as shown in curve Y-B, in the low temperature working fluid. The process described above is repeated for each Stirling cycle.

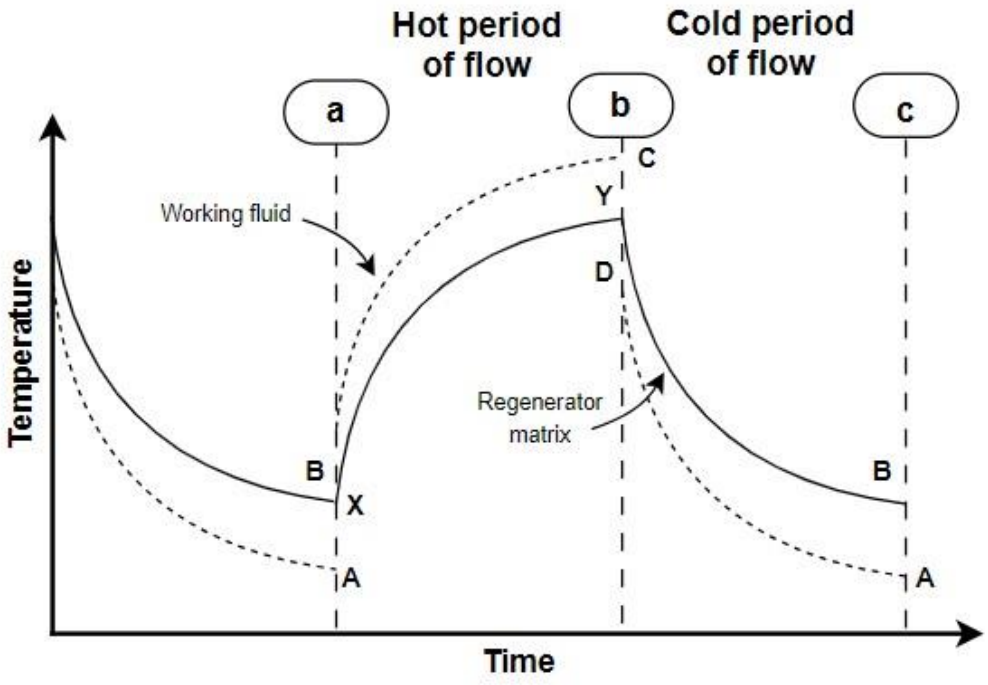

Fig. 8 Regenerator temperature fluctuation during Stirling cycle

To obtain great heat storage capacity, manufacturing materials such as fibrous wires, layers of metal gauzes, mesh and packed balls made of copper, nickel, chrome nickel and others conductive metals are used. To improve the heat transfer coefficient between the matrix and the working fluid, the following characteristics should be properly combined to improve the regenerator efficiency. As can be easily understood, each of the following characteristics requires a different type of regenerator. Therefore, a middle ground solution for the selection of the regenerator is needed.

Requirements	***Type of regenerator***
For greater thermal conductivity	Bigger capacity, compact plexus
For minimum flow losses	Smaller capacity, porous plexus
For minimum unused gap	Smaller capacity, dense plexus
For maximum heat transfer	Bigger capacity, distributed plexus
For minimum pollution	Plexus of minimum flow obstruction

Table 2

2.2.6 Non-Ideal adiabatic analysis

Analysis of Stirling cycle as described above was carried out under assumptions, such as perfect regeneration, that needed to be taken into consideration in order to reach a mathematical approach. Hence, it would be reasonable that theoretical results would deviate from actual engine cycle. The purpose of this section is to identify a number of factors that cause this discontinuity between theoretical and experimental results. W. Martini provides an analysis which evaluates the effects of various factors based on theoretical and experimental results of GPU-3 B-type Stirling engine [10], [11]. With due consideration of this analysis, thermal and frictional losses of the Stirling cycle are evaluated. By adding these losses in ideal adiabatic model, the non-ideal adiabatic model is derived which is used for the CCHP system.

Flow Friction Losses

Initially, basic power output of the engine is computed as if there are no frictional losses. Then, the total energy loss due to fluid friction is deducted from the basic power. Engines with energy losses that tend to be less than 10% of the basic power shall be deemed to be accepted.

Fluid friction inside engine's porous media and tubes can be computed by published correlations for steady, fully developed flow of working gas. Comparing the amount of the gas inventory found in hot spaces and cold spaces with crank angle, a good description of periodic flow can be approximated by 4 discrete steps in a sequence. Starting with (1) steady gas flow in one direction, (2) no flow for a period of time, (3) then steady flow at the opposite direction and (4) continuing with no flow to complete a cycle. Mass flow through regenerator is not quite in phase due to accumulation and depletion of mass inside it. Gas density changes during Stirling cycle, resulting in a greater mass flow at the cold end rather than the mass flow at the hot end. The average mass flow rate and the average friction of a complete cycle time where gas flow direction is at the hot end of the regenerator is used so as to calculate flow friction due to the heater and the amount of heat transferred. In similar manner, average mass flow rate and the average percentage of a complete cycle time where gas flows to the opposite direction at the cold end of the regenerator is used for cooler flow friction and heat transfer computations. Regenerator's equations utilize mean values of the above flows and time frictions of both directions.

Regenerator pressure drop:

$$DP = \frac{F \cdot G^2 \cdot LR}{2 \cdot 10^7 \cdot RH \cdot RHOM} \tag{42}$$

Where,

F: matrix flow friction factor
G: mass velocity in regenerator, $g/sec\ cm^2$
LR: length of regenerator, cm
RH: Hydraulic radius of regenerator, cm
$RHOM$: mean density value of gas, $g/\ cm^3$

Heater and Cooler pressure drop:

$$DP_i = \frac{2 \cdot F \cdot G_i^{2^2} \cdot L_i}{10^7 \cdot DI_i \cdot RHOM} \quad where\ i = \begin{cases} H, & for\ heater \\ C, & for\ cooler \end{cases} \tag{43}$$

Where,

F: friction factor for tubes
G_i: mass velocity in heater, cooler, $g/sec\ cm^2$
L_i: total length of heat exchanger tubes, cm
DI_i: internal inside of tubes, cm
$RHOM$: mean density value of gas, $g/\ cm^3$

Heater and cooler pressure drops tend to be less than regenerator due to smaller size. Size and design of heat exchangers should serve engine's needs for heating and cooling. So, no path of designing a heat exchanger is certain. Interleaving fins heat exchanger has the advantage that gas flows into rather than through it, causing better heat transmission. Although, it is complicated because the flow passage area changes with stroke. The analysis from which we derived the equations above, assume steady and fully developed flow. Hence, small diameter, round tubes are chosen so as to make heat transfer more efficient.

For larger Stirling engines, it would be more accurate to divide the regenerator and even heater and cooler exchangers which are smaller into sections. By doing so each section would be examined separately and evaluate the mass flow and temperature for every time step. Finally, the pressure drop and flow loss in each section can be summed to evaluate total energy loss.

The overall pressure drop is calculated by summing the pressure drops of all heat exchangers. The product of total pressure drop in MPa and the volumetric flow rate in cm^3/sec gives the total energy loss in $Watts$.

$$WP_i = \frac{2 \cdot DP_i \cdot WS_i \cdot FCT_i}{RHOM} \qquad where\ i = \begin{cases} H, for\ heater \\ R, for\ regenerator \\ C, for\ cooler \end{cases} \tag{44}$$

Where,

WP_i: flow friction loss, W
DP_i: pressure drop, MPa
WS_i: effective flow rate, g/s
FCT_i: fraction of time flowing into heat exchangers
$RHOM$: mean density value of gas, g/cm^3

Mechanical Friction Loss

Mechanical loss is the difference between indicated and brake power of the engine. It is hard to calculate this loss accurately due to various factors such as bearings, seals, lubrication, and temperature which affect engine operation. As a result, there is no certain equation that can describe this kind of friction loss reliably and essentially must be measured. However, if the engine itself were used, the mechanical loss would be combined with power delivered by the engine and would not be detected. The friction loss should be measured directly by having the engine operate at the design average pressure with a very large dead volume so that very little engine action is possible. However, an empirical principle that is usually applied in such a case where experimental tests aren't feasible, is that this kind of friction consists of 20% of total engine's power output.

Heat Losses

To estimate the initial amount of heat supplied from the heat source, the heat losses that occur as the engine operates are examined. In this way, actual heat input in the engine is evaluated by subtracting every heat loss from the total amount of heat energy supplied from combustion system. In addition, performance of stirling engine is computed. Once heat losses are known, the total amount of fuel supplied at the CCHP system could be evaluated. In the section below, basic heat losses along with reasons causes them are investigated and described individually.

Reheat Loss

Ideal regeneration cannot be achieved in actual operation. Hence, the amount of heat stored by the regenerator is partially returned to the working gas as it flows to the hot space. The remaining amount of heat that is not returned back to the working fluid is supplied by means of the engine's heat source as extra heat input. Figure 8 shows how the flow of the gas during cycle affects gas temperature in the heat exchangers. It is observed that gas attains cooler temperature as reaches cold space. However, as the gas flows back to the hot space is heated up partially until point C. This temperature difference between the hot space and the gas entering from regenerator is multiplied by the heat capacity, the effective flow rate and the fraction of time that this gas is flowing so as to calculate reheat loss.

$$QRH = FCT \cdot WRS \cdot CV \cdot (THM - TCM) \cdot \frac{2}{NTUV+2} \quad (45)$$

Where,

FCT: fraction of time flowing into hot space
WRS: effective flow rate, $g/\ s$
CV: heat capacity at constant volume, $j/\ kg\ K$
THM: effective temperature of hot space, K
TCM: effective temperature of cold space, K
$\frac{2}{NTUV+2}$: regenerator's ineffectiveness factor

The equation above provides a good approximation of reheat loss. Fraction of time where gas flowing into hot space is estimated by extrapolating the maximum cycle time that this process would take if gas flow was always at its maximum value. This value is usually estimated about one-third. However, if a numerical approach is used, fraction of time could be computed when flow resistances are calculated provided that periodic flow can be approximated by 4 discrete steps in sequence that mentioned previously. The calculated gas flow through regenerator equals the effective flow rate. If variable gas flow occurs from regenerator to hot space, then fraction of time is divided in time slots so reheat loss is evaluated separately and summed to calculate total reheat loss for the cycle.

Shuttle Conduction

Construction material of displacer is heat conductive and because of its placement contributes to heat transmission between hot and cold space of the engine. Shuttle conduction occurs when a displacer oscillates across a temperature gradient. Displacer absorbs heat during the hot end of its stroke and dissipates heat during cold end of its stroke. Hence, the effectiveness of the Stirling cycle is slightly reduced. As the process evolves, temperatures of displacer and cylinder wall do not significantly change. Shuttle conduction loss depends on several factors such as temperature gradient $(THM - TCM)/LD$ between hot and cold space, gas thermal conductivity, displacer stroke and clearance gap around displacer.

$$QSH = \frac{1+LB}{1+LB^2} \cdot \frac{\pi}{8} \cdot \frac{SD^2 \cdot KG \cdot (THM-TCM) \cdot DCY}{GR \cdot LD} \tag{46}$$

Where,

LB: temperature wavelength, cm
SD: stroke of displacer, cm
KG: gas thermal conductivity, $W/cm\ K$
DCY: inside diameter of engine cylinder, cm
THM: effective temperature of hot space, K
TCM: effective temperature of cold space, K
GR: clearance gap around displacer, cm
LD: length of displacer, cm

It should be emphasized that above equation is applicable for chiefly sinusoidal motion of displacer. This statement is in agreement with Schmidt assumption of sinusoidal volumes variations.

Static Heat Conduction

This type of heat loss refers to the transfer of heat from hot to cold parts of the engine through both the working gas and conductive metal components. Heat is transferred by means of conduction and radiation. Static heat conduction occurs regardless of the engine's speed or whether it is currently in use as long as the engine remains hot. At the regenerator, this type of loss is evaluated as if the accumulated gas were stagnant.

There are 3 main losses which are related to displacer engine component:

1. Thermal conductivity of displacer's cylinder wall.
2. Thermal conductivity of displacer's clearance gap.
3. Thermal conductivity of displacer's stored gas.

Those three losses are evaluated using the following equation with the terms replaced each time based on the type of computed loss. When computing displacer's cylinder wall loss, the K term represents the thermal conductivity of metal. Otherwise, it represents thermal conductivity of working gas. The total thermal conductivity of displacer is evaluated by adding the above losses.

$$QC_{1,2,3} = \frac{K \cdot AHT \cdot (THM - TCM)}{LD} \tag{47}$$

Where,

K: thermal conductivity of metal or gas, $W/cm\,K$
AHT: cylinder wall heat transfer surface area, cm^2
THM: effective temperature of hot space, K
TCM: effective temperature of cold space, K
LD: length of displacer, cm

At heat transfer areas where volume varies during engine cycle, thermal conductivity changes significantly. In such a case, the area is divided in smaller zones and heat conduction is examined independently. Thus, temperature and average heat conduction is computed so as to assign the corresponding thermal conductivity. In addition, thermal conductivity of a component depends on the material that is made of. Following the above method, we divide cylinder and regenerator wall in 3 separate zones for our engine. Thermal resistance of each zone is evaluated and is used in the following equation. The number of cylinders and regenerators that the engine consists of, is represented by NR term. In case of computing thermal conductivity of cylinder's wall, NR term equals 1 due to B-type configuration that has been selected for our model. Else, if thermal conductivity of regenerator's wall is been calculated, NR term has been chosen to be 8 for our model.

$$QC_{4,5} = \frac{(THM-TCM)}{R_1+R_2+R_3} \cdot NR \tag{48}$$

Where,

R: component's thermal resistance, K/W
NR: number of cylinders or regenerator components
THM: effective temperature of hot space, K
TCM: effective temperature of cold space, K

Regenerator matrix is mainly made of metal gauzes and fibrous wires. Many layers of the aforementioned materials are used in series so as to store as much heat as possible. Although, the degree of layering affects thermal conductivity of each layer since the controlling resistance is the contact between adjacent wires. Hence, following equation evaluates conduction through regenerator matrices.

$$QC_6 = \frac{NR \cdot KMX \cdot AHT \cdot (THM-TCM)}{LR} \tag{49}$$

Where,

KMX: thermal conductivity of regenerator matrix, $W/cm\,K$
NR: number of regenerator components
AHT: regenerator heat transfer surface area, cm^2
THM: effective temperature of regenerator hot space, K
TCM: effective temperature of regenerator cold space, K
LR: length of regenerator, cm

Displacer of Stirling engines is usually hollow. As a result, heat is transferred through radiation and gas conduction across this space. Radiation heat transport follows the above formula. With consideration of engine's specifications, area factor of radial heat transfer, emissivity factor and radiation shield factor are determined so as to compute total radiation along cylinders.

$$QR = FA \cdot FE \cdot FN \cdot AHT \cdot SI \cdot (THM^4 - TCM^4) \tag{50}$$

Where,

FA: area factor of radial heat transfer
FE: emissivity factor
FN: radiation shield factor
AHT: cylinder heat transfer surface area, cm^2
SI: Stefan-Boltzmann constant $5.67 \cdot 10^{-12},\ W/cm^2K^4$

By adding up the above static heat losses that occur at the different parts of the engine, the total static heat conduction loss is evaluated.

$$QC_{total} = QC_1 + QC_2 + QC_3 + QC_4 + QC_5 + QC_6 + QR \tag{51}$$

Pumping Loss

Due to engine manufacture, a radial gap exists between the engine cylinder's ducts located at the cold space and displacer's manifolds. This gap causes pumping loss, which is proportional to the engine frequency. As the engine pressurizes and depressurizes so as to transfer the working fluid, gas flows into and out of this gap. Since the radial gap is located at the cold space of the engine, the temperature of the gas flowing out of it remains low, requiring additional heat to compensate for this heat loss.

$$QPU = \left(\pi \cdot \frac{DCY}{KG}\right)^{0.6} \cdot \frac{2 \cdot LD \cdot (THM - TCM)}{1.5 \cdot Z_1} \cdot \left[\frac{(PC_{max} - PC_{min}) \cdot NU \cdot CP \cdot 2}{(THM - TCM) \cdot \frac{R}{MW}}\right]^{1.6} \cdot GR^{2.6} \quad (52)$$

Where,

DCY: cylinder diameter, cm
KG: thermal conductivity of gas, $W/cm\ K$
LD: length of displacer, cm
Z_1: compressibility factor of gas
PC: engine pressure, MPa
NU: engine frequency, Hz
CP: gas specific heat capacity at constant pressure, $kj/kg\ K$
MW: molecular weight of gas, $g/\ mol$
R: universal gas constant 8.314, $J/mol\ k$
GR: clearance around hot cap, cm

Temperature Swing Loss

The oscillation of the regenerator matrix temperature was considered negligible when computing the reheat loss. However, in certain instances, temperature fluctuation is substantial during engine cycle. Temperature swing loss represents the additional heat supplied from heat source due to finite heat capacity of regenerator. Firstly, temperature drop of the regenerator is calculated in order to assess the additional heat that is required. The temperature swing in regenerator's matrix, occurring during the fraction of time when the gas flows from the cold to the hot space, is determined as follows:

$$TS = \frac{WRS \cdot C_v \cdot FCT \cdot (THM - TCM)}{NU \cdot MX \cdot CPM} \quad (53)$$

Where,

TS: matrix temperature swing during one cycle, K
WRS: mass flow through regenerator, g/sec
C_v: specific heat capacity at constant volume, $kj/kg\ K$
FCT: fraction of cycle time flow is into hot space
MX: mass of regenerator matrix, kg
CPM: heat capacity of regenerator metal, $kj/kg\ K$

Half of the above computed value, i.e. $TS/2$, equals temperature difference of cold and hot space multiplied by regenerator ineffectiveness in reheat loss equation since it has zero value at the start of the flow and grows until TS. Considering the aforementioned, the following formula is used to calculate the temperature swing loss:

$$QTS = FCT \cdot WRS \cdot C_v \cdot \frac{TS}{2} \tag{54}$$

Where,

FCT: fraction of cycle time flow is into hot space
WRS: mass flow through regenerator, g/sec
C_v: specific heat capacity at constant volume, $kj/kg\ K$

The overall thermal and frictional losses are summed up by the aforementioned equations. The non-ideal adiabatic model of Stirling engine is derived from ideal adiabatic analysis including above losses. In that way, representative values of heat energy supplied in CCHP system and work done by the prime mover are estimated. The actual heat input Q_{ach} is derived by adding engine thermal losses to the base heat input calculated by ideal adiabatic analysis. Similarly, the total amount of heat dissipated Q_{ack} is calculated. In terms of the fuel's heating value, the rate at which the fuel is consumed to provide the required amount of thermal energy is estimated.

$$Q_{ach} = (Q_h \cdot fr) + (QRH + QSH + QC_{total} + QPU + QTS) \tag{55}$$

$$Q_{ack} = (Q_k \cdot fr) + (QRH + QSH + QC_{total} + QPU + QTS) \tag{56}$$

$$Q_{ach} = M_{FF} \cdot HHV \tag{57}$$

The actual work done is evaluated, by subtracting frictional losses occurring during engine cycle. In addition, taking into account the efficiency of the electric generator n_g, the mechanical power converted into electrical power is evaluated.

$$P_{mech} = (W \cdot fr) - (WP_h + WP_r + WR_k + MFL) \tag{58}$$

$$P_{el} = n_g \cdot P_{mech} \tag{59}$$

The recovered amount of dissipated thermal energy (Q_{ack}) is then provided for heating and cooling applications. The Usage Factor Coefficient (uf) determines the percentage of thermal energy that will be provided in each application, taking into account the building load profile, operating costs, and other constraints. In addition, hw_c factor determines the percentage of the provided thermal energy used to heat water.

Provided for cooling: $$Q_g = uf * Q_{ack} \tag{60}$$

Provided for heating: $$Q_{hw} = hw\_c * (1 - uf) * Q_{ack} \tag{61}$$

2.3 Hot Water Storage Tank

A storage tank is used to meet the thermal needs of the building by providing hot water. Low temperature water is heated using a percentage of the waste heat from the prime mover. Once the water has been heated, it is stored in a tank so that it is available when it is needed. In the system being examined, no thermal losses have been taken into account, such as the heat transfer loss and the thermal loss of the storage tank over time. In this way, the recovery of waste heat is achieved where in other cases it would be lost to the environment.

The amount of heat energy input into the system is a function of a number of parameters simultaneously. More specifically, the percentage of thermal energy provided for water heating is determined by a usage factor that takes into account the current hot water demand and remaining hot water.

Technical parameters that must be specified for the operation of the storage tank are reference temperature of hot water and tank capacity. The capacity of the storage tank will be selected in accordance with the daily hot water demand in relation to the building's specifications. In addition, in most cases, the hot water reference temperature for such applications is set at around 60°C.

Once the amount of thermal energy supplied to the system is determined in combination with the above, the mass flow of water to be heated is evaluated using the specific heat formula as follows:

$$m_{hot\,water}^{inlet} = \frac{Q_{hot\,water}}{C_p \cdot (T_{ref} - T_{urb})} \tag{62}$$

The next section outlines operational assumptions for the case study under consideration, including the minimum and maximum water container capacity, and other assumptions under which the storage tank operates. The Eq. (63) simulates the use of hot water from storage tank for every period of time which is expressed as follows:

$$SW = SW + \sum \left\{ m_{hot\,water}^{inlet} - m_{hot\,water}^{outlet} \right\} \cdot dt \tag{63}$$

2.4 Absorption Chiller

Absorption chillers are thermally activated systems that provide cooling without the need of high electric power. Solar, geothermal and waste heat are the most common environmental friendly sources of energy that can be used as a heat input. Nevertheless, conventional heat sources such as fossil fuel combustors could be also used. The opportunity of energy savings that provides the use of such a system when heat source is available, has grown the interest of many researchers. Thus, the development of aforesaid systems at any size so as to cover the cooling demands for industrial, commercial and residential use is under investigation.

The main idea of the absorption systems is to replace mechanical compression at conventional systems that is energy consuming. The use of mechanical compression is to pressurize the vaporized refrigerant. This work is replaced by the absorber-generator system which is used to

absorb and then pressurize the refrigerant vapor. This is achieved with the use of a working pair consisting of a refrigerant and a solution which can absorb the refrigerant. The most common solution pairs are LiBr-water and water-ammonia. [12]

Refrigeration is produced by evaporating or vaporizing a volatile medium. Volatile media have the property of rapidly increasing vapor pressure with temperature variation. Therefore, they appear to have a high vapor pressure even at ambient temperatures. This results in their evaporation under ambient conditions, absorbing at the same time heat from the surrounding space with the end result of cooling it. The volatile media used in the production of refrigeration are known as refrigerants.

2.4.1 Solution Pairs

Thermodynamic properties of refrigerant which is used in solution determines the temperature range in which chiller is properly operates. More specifically, water refrigerant is suitable for cases where evaporation temperature is above 0 °C, such as air-conditioning. On the other hand, ammonia boils at -33 °C at atmospheric pressure and can be used for minus temperatures cooling demands. However, higher temperature of heat source needed when using ammonia-water rather than using LiBr-water pair. [13]

The fluid pairs selection should meet several requirements in order to achieve a good thermodynamic system performance, which are:

1. Non-solid phase. Neither refrigerant nor the absorbent should form a solid phase as temperature and composition of the solution change. That would cause either restricted or no flow at all.

2. Fluid's pressure. Moderate operating pressure should be used between high and low pressure chambers so as to reduce the electrical power demand of the pump which is used for the fluid circulation.

3. Volatility ratio. In the generator, the refrigerant should be easily separated from absorbent only by heating the solution.

4. Affinity. Since a mechanical compression is replaced by solution pair, refrigerant should be strongly attracted by absorbent in order to achieve absorption cycle.

5. Chemical stability is needed so as to prevent undesirable formation of solids or corrosive substances that would make chiller deviate from proper operation.

Absorption chiller in the proposed CCHP system is used for air-conditioning purposes. Considering the limited waste heat temperature used as a heat source of absorption chiller, in combination with above fluid's requirements, the LiBr-water solution has been chosen as the most appropriate option.

2.4.2 Single effect absorption cycle

Absorption chiller consists of five main modules, i.e. absorber, generator, condenser, evaporator and a heat exchanger the use of each one will be discussed below along with absorption cycle. Also, it is classified by the method of heat supply and whether the absorption cycle is single or double effect. Double effect systems include an additional stage of absorption that acts as a topping cycle on the single effect cycle. The heat rejected from the high temperature stage is used to power the lower temperature stage. These systems provide a higher coefficient of performance in comparison with single stage. However, higher temperature heat sources are needed so both stages of absorption can operate simultaneously. A schematic presentation on a pressure-temperature diagram for a single effect LiBr-water absoprtion cycle is presented in Figure 9. [13]

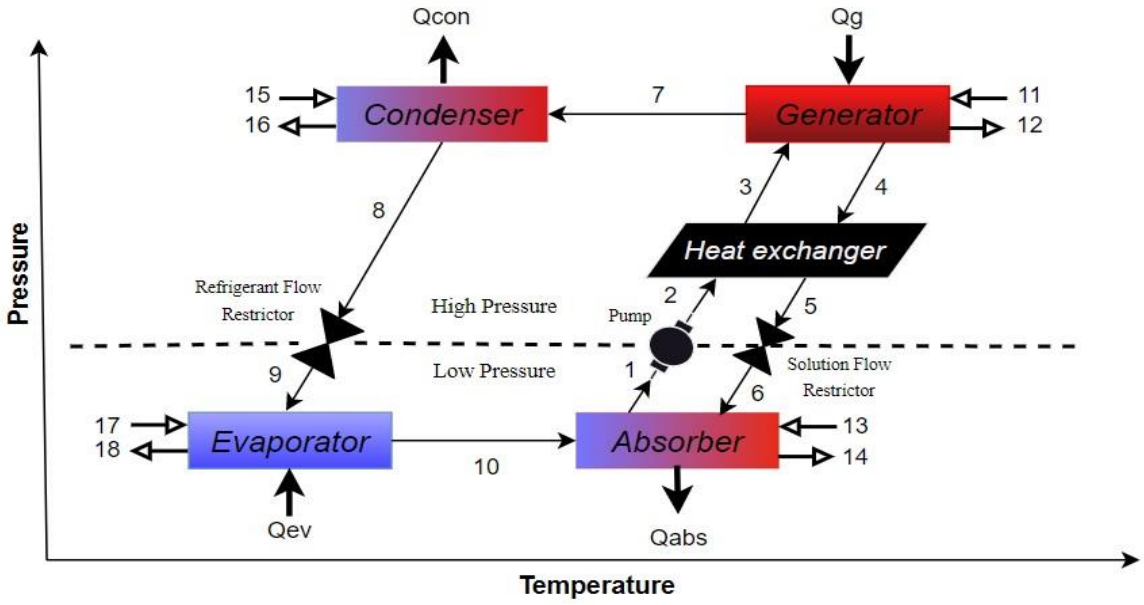

Fig. 9 Single effect, LiBr-water absorption cycle

Starting from point (1) of the above figure, weak solution is pumped (2) from the absorber to the generator (3) by means of preheat exchanger. Pump is needed to transfer the fluid due to pressure transition from low to high value. In the heat exchanger, a part of the weak solution is mixed with strong solution which flows to the opposite direction. The purpose of this mixture is to reduce temperature and concentration of strong solution in order to prevent crystallization as it enters the absorber.

In the generator, waste thermal energy of CCHP system is utilized and boils the refrigerant off the solution. Due to high volatile ratio and pressure of the generator, refrigerant change to vapor form while absorbent remains liquid. Once the refrigerant and the absorbent are separated, refrigerant vapor flows to the condenser (7). Strong solution exits the generator (4) and is cooled in the heat exchanger before reaching the absorber.

As soon as vapor reaches condenser chamber, heat is rejected as the refrigerant condenses. It is worth noted that condenser and absorber share an individual cooling system that maintains their temperature constant by circulating water. The cooling water inlet temperature depends on the available method of cooling water, which may be a cooling tower or a well. Flow restrictor helps the condensed liquid (8) flows from high pressure chamber to low pressure evaporator (9).

Tubes located in the evaporator circulate water at room temperature which provides heat from the load. Evaporator has a very low pressure (vacuum) due to intense attraction of the refrigerant from the absorbent. As a consequence, boiling point of refrigerant is reduced and evaporates immediately once saturated liquid come into contact with evaporator's tubes. In this way, cooling effect occur and water temperature reduced.

In the absorber, the strong solution provided by the heat exchanger (6) attracts the evaporated refrigerant (10). When the two fluids come into contact, heat is emitted and needs to be removed. Therefore, weak solution is sprayed over the water loop tubes of the cooling system, which are shared with the condenser, so as to remove the unwanted heat. Finally, a complete absorption cycle has occurred and the mixture of refrigerant-absorbent solution is returned to the heat exchanger for the next cycle.

A pressure- temperature graph is presented in Figure 10 where the diagonal lines represent constant LiBr mass fraction. The pure water line located at top left and the strong solution line at top right. This graph is also known as the Duhring chart. [13]

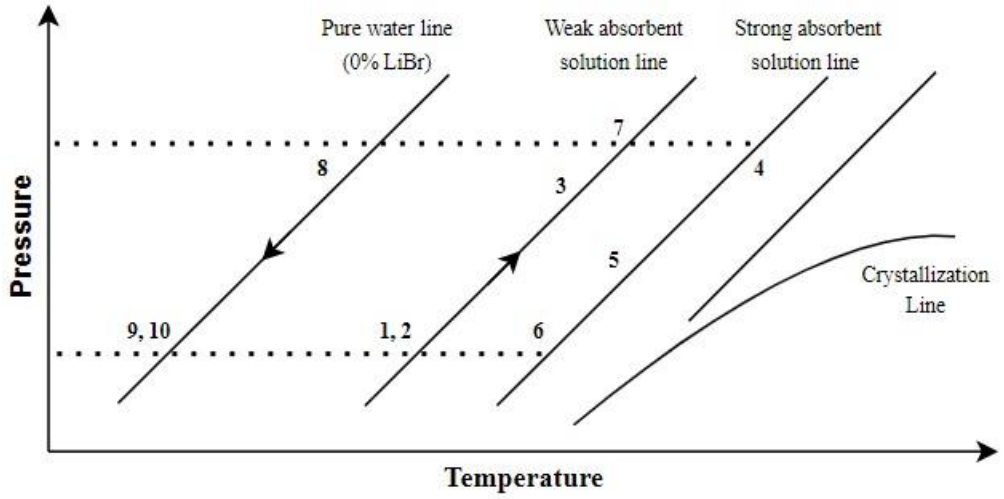

Fig. 10 Duhring chart of the LiBr-water absorption cycle

A schematic presentation of a single-effect LiBr water absorption chiller as described above is shown in the next figure. This scheme illustrates the chiller's structure in further detail. Thus, in addition to the main modules of the absorption chiller, this diagram also illustrates the cooling

tower of the condenser and absorber. It also shows the flow of the solution pair through the different components and the hot and cold water loops in the generator and evaporator, respectively. [14]

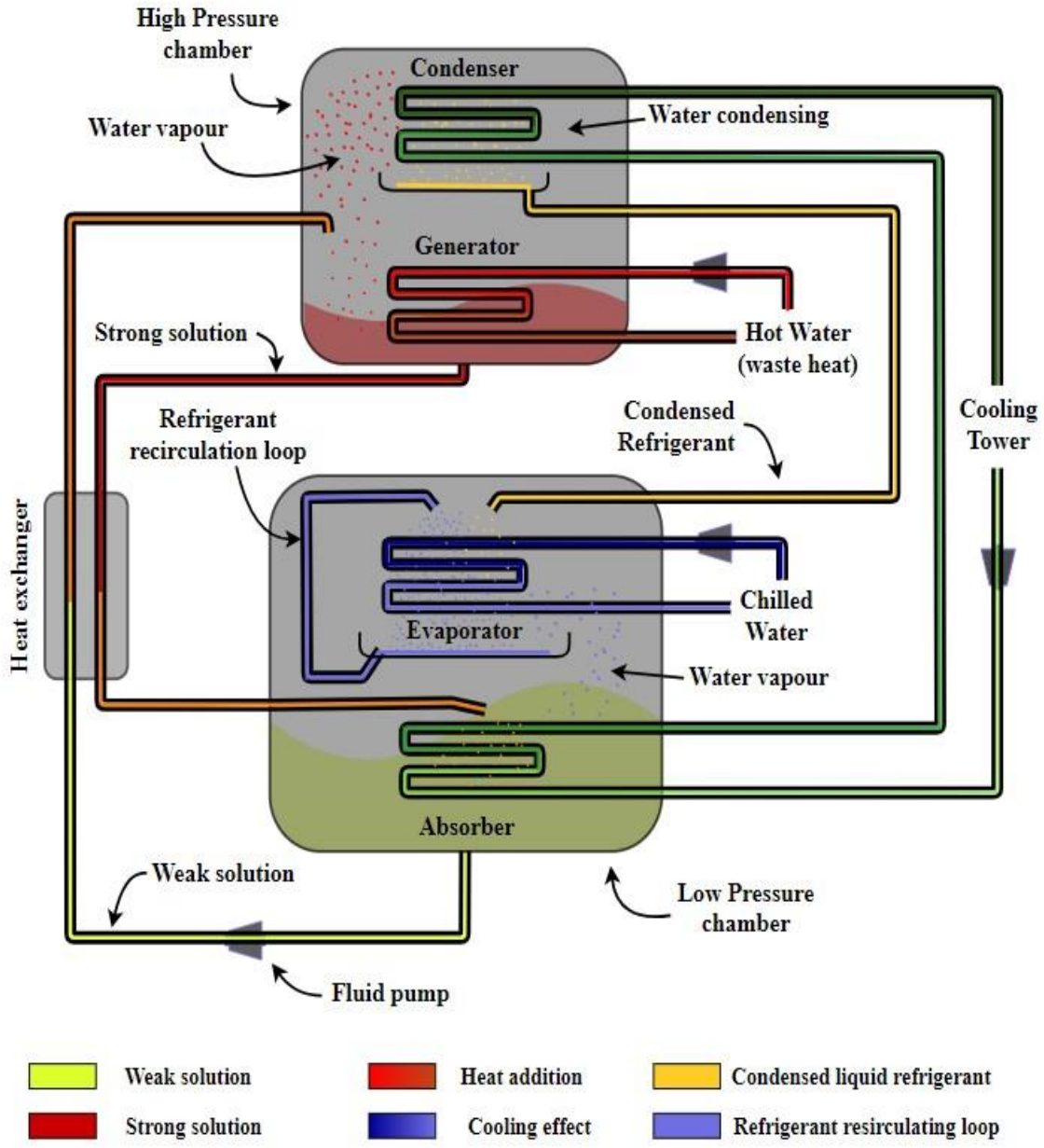

Fig. 11 Single effect LiBr-water absorption chiller stcheme

2.4.3 Crystallization

Lithium Bromide absorbent is a salt and has a crystalline structure. There is a specific minimum solution temperature depending on the absorbent concentration when LiBr is dissolved in water refrigerant. Below this temperature, salt begins to crystallize and separate from the solution pair. [13], [15], [16]

Crystallization occurs when LiBr concentration is too high or the solution temperature is too low. At the outlet of the solution heat exchanger, solution has the highest absorbent concentration of any of the other points with the lowest temperature, simultaneously. As a reult, there is a high probability of crystallization at this point. In such situation, heat should be added in order to raise the solution temperature until salt crystals return to liquid form. Considering the above, the effectiveness of the solution heat exchanger is limited by the minimum temperature the solution should have as it flows to the absorber.

A high load of thermal energy in the generator would cause the absorbent concentration in the solution to increase above the crystallization point. Another factor contributing to crystallization is an increase in evaporator pressure due to air leakage into the chiller, which rises the evaporation temperature. Therefore, periodic evacuation at the evaporation chamber as a maintenance procedure is critical.

Excessively low temperature of cooling water at the condenser combined with high thermal energy load in the generator could lead to salt crystallization. This would be prevented by controlling cooling tower water temperature provided at the condenser in relation to thermal load and ambient temperature. This keeps condenser cooling temperatures close to ambient temperature. However, in such a case, the temperature of the weak solution entering the solution heat exchanger may be low enough to partially cool the high temperature strong solution returning from the generator.

The machine goes through a dilution cycle during a typical shutdown. The reason is to reduce the concentration of the solution throughout the chiller and prepare the fluid reach ambient temperature without crystallization. As a result, abruptly stopping the chiller operation would lead to absorbent crystallization, especially if it is operating at high load conditions where the solution concentration is high.

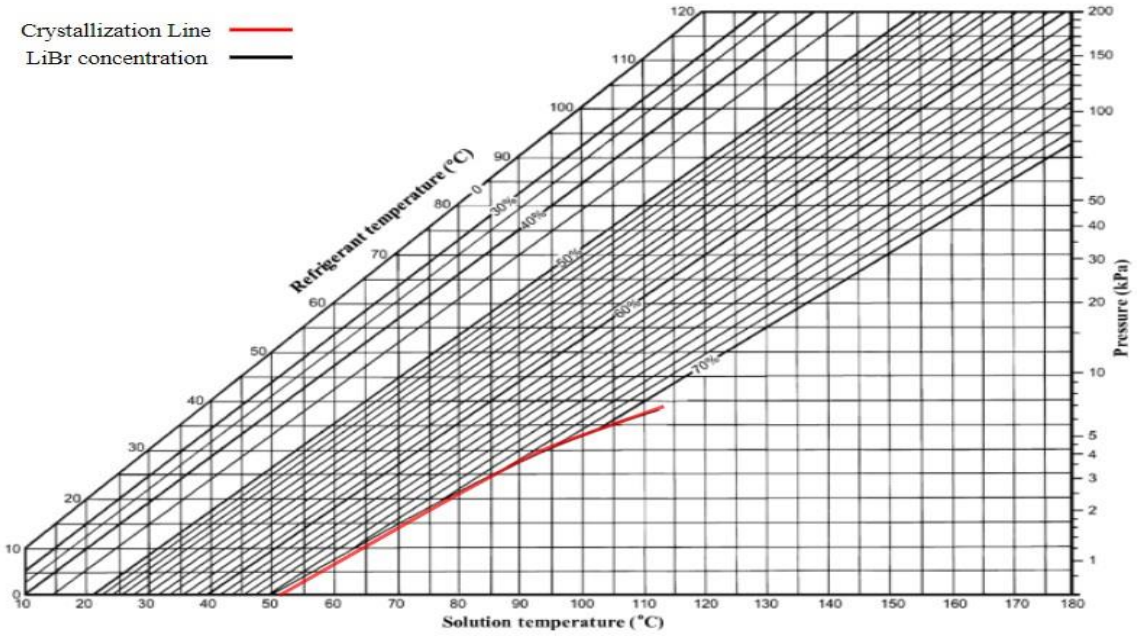

Fig. 12 Equilibrium chart for LiBr solution with crystallization curve

2.4.4 Thermodynamic analysis

To perform a thermodynamic analysis of the system, basic assumptions for the operation of the absorption cycle should be considered depending on absorption classification. Basic assumptions applied in this case where a single-effect LiBr-water absorption chiller is used are: [14]

- Refrigerant consists of pure water.
- There are no pressure changes at any component except the flow restrictor and pump.
- The refrigerant completely boils off the solution in the generator. As a result, at points 1, 4 and 8 there is only saturated liquid.
- There is only saturated steam in the evaporator, which passes through point (10), so point (11) can be neglected.
- Flow restrictors are adiabatic.
- Pump is isentropic.
- There are no jacket and transmission heat losses.

For the thermodynamic analysis of the absorption system the principles of mass conservation and first law of thermodynamics are applied at every system's component separately. In the analysis, each component is considered as an individual control volume with inlet and outlet streams, heat transfer and work interactions. In the system, total mass conservation includes the mass balance of both solution substances, i.e. refrigerant and absorbent. The governing equations for mass balance and concentration of absorbent are: [12], [13], [14]

$$\sum \dot{m}_i - \sum \dot{m}_o = 0 \tag{64}$$

$$\sum (\dot{m}x)_i - \sum (\dot{m}x)_o = 0 \tag{65}$$

Where $\dot{m}$ is the mass flow rate and x is mass concentration of absorbent in the solution. Also, i and o indicators denote to inlet and outlet streams, respectively. Energy balance for every system component is derived from the first law of thermodynamics as follows:

$$\sum (\dot{m}h)_i - \sum (\dot{m}h)_o + [\sum Q_i - \sum Q_o] + W = 0 \tag{66}$$

Where h_i and h_0 are the component's enthalpy stream. In addition, Q_i, Q_o are inlet and outlet heat flow and W the internal work of each component.

However, the energy balance is applied not only to each component, but to the system as a whole. Hence, the thermal energy of the four main components should sum to 0. Assuming that the pump work and environmental energy losses of the absorption chiller are insignificant, the equation describing the total energy balance is:

$$Q_C + Q_A = Q_G + Q_E \tag{67}$$

Thermodynamic characteristics of water refrigerant and LiBr absorbent, i.e. pressure, temperature and enthalpy, are estimated as a function of solution concentration and other input variables. By

using published mathematical correlations for fluid properties, water and LiBr properties are determined at different operating points of absorption chiller. Once the thermodynamic properties of the solution are estimated, absorption analysis is applied to all system components to evaluate mass and energy for every chiller component. [17], [18]

Heat Exchanger

Solution heat exchanger is used to recover some of the heat as strong solution flows from generator to absorber and return it as weak solution flows in the opposite direction. The heat exchanger efficiency is given as an input parameter for calculating temperature of weak and strong solution. Temperature indices follow the enumeration of Figure 9.

$$Eff_{HX} = \frac{T_4 - T_5}{T_4 - T_2}$$

Using heat exchanger efficiency, inlets and outlets mass flow temperatures are evaluated. Enthalpy is estimated with regard to LiBr mass fraction and temperature. Once the enthalpy at each point is known, a relationship is derived between the masses of the weak and strong solution pair.

Mass balance: $m_2 = m_3 \ , \ m_5 = m_6$

Energy balance: $Q_{HX} = \dot{m}_2 h_2 + \dot{m}_4 h_4 = \dot{m}_3 h_3 + \dot{m}_5 h_5$

Generator

Mass balance is used to derive a relationship between the mass flow entering and leaving the generator. In addition, taking into consideration the heat exchanger energy balance equation above, a two equation system is carried out. In this manner, inlet and outlet mass flows can be evaluated, since Q_g is the input thermal energy corresponding to the waste heat of the prime mover.

Mass balance: $\dot{m}_3 = \dot{m}_4 + \dot{m}_7 \ , \ \dot{m}_3 x_3 = \dot{m}_4 x_4 + \dot{m}_7 x_7$

Energy balance: $Q_g = \dot{m}_4 h_4 + \dot{m}_7 h_7 - \dot{m}_3 h_3$

Condenser

Condenser has one inlet and one outlet stream from generator and evaporator, respectively. As a result, mass flow and concentration of the refrigerant remain the same.

Mass balance: $\dot{m}_7 = \dot{m}_8 \ , \ x_7 = x_8$

Energy balance: $Q_c = \dot{m}_7 (h_7 - h_8)$

Evaporator

As was mentioned in assumptions under which the thermodynamic analysis is performed, saturated liquid entering the evaporator is vaporized completely. Therefore, there is no liquid left to pass through tube (11) and consequently $m_{11} \approx 0$.

Mass balance: $\dot{m}_9 = \dot{m}_{10} + \dot{m}_{11}$

Energy balance: $Q_e = \dot{m}_{10}h_{10} + \dot{m}_{11}h_{11} - \dot{m}_9 h_9$

Absorber

Mass fractions x_1 and x_6 represent weak and strong solution, respectively. They are calculated with respect to solution temperature and saturation pressure. Specific volume of the weak liquid solution passing through pump does not change from point (1) to (2), consequently $\dot{m}_1 = \dot{m}_2$. The same applies for strong solution which flows via solution flow restrictor from heat exchanger to absorber, i.e. $\dot{m}_5 = \dot{m}_6$.

Mass balance: $\dot{m}_1 = \dot{m}_{10} + \dot{m}_{11} + \dot{m}_6$, $\dot{m}_1 x_1 = \dot{m}_6 x_6$

Where x_{10}, x_{11} are 0 due to zero concentration of LiBr in the fluid coming from evaporator. Heat transfer in the absorber can be determined since all variables of the equation are known.

Energy balance: $Q_a = \dot{m}_{10}h_{10} + \dot{m}_{11}h_{11} + \dot{m}_6 h_6 - \dot{m}_1 h_1$

A way to verify the accuracy of the obtained results is system's energy balance. More specifically, thermal energy rejected to the environment via condenser and absorber. On the other hand, thermal energy supplied to the generator and evaporator. From the first law of thermodynamics the sum of the above should be equal to 0.

Coefficient of performance

The cooling COP of the absorption system is defined as the heat load in the evaporator per unit of heat load in the generator. With respect to Figure 9 enumerations, the COP of the single effect LiBr-water absorption chiller is estimated:

$$COP_{cooling} = \frac{Q_e}{Q_g} = \frac{\dot{m}_{10}h_{10} - \dot{m}_9 h_9}{\dot{m}_4 h_4 + \dot{m}_7 h_7 - \dot{m}_3 h_3}$$

2.5 Building Thermal Loads Modelling

In this work, each building is divided into thermal zones. A thermal zone is a section of a building that allows independent control of its internal temperature and has its own characteristic thermal behavior. Using the following thermal equilibrium equation, a mathematical relationship between the internal temperature, thermal gains, thermal loads and ambient temperature can be developed in order to analyze the thermal behavior of each thermal zone [19], [20].

$$p_z \cdot C_z \cdot V_z \cdot \frac{dT_{in,z}}{dt} = \dot{Q}_{ex,wall,z} + \dot{Q}_{in,wall,z} + \dot{Q}_{win,z} + Q_{in,z} + \dot{Q}_{sw,z} + \dot{Q}_{sg,z} - Q_{ev,z} \quad (68)$$

The heat exchange between a thermal zone and its outdoor environment is described by Equations (69) -(72), while Equation (73) estimates the heat exchange between a thermal zone and its neighboring zones.

$$\dot{Q}_{ex,wall,z} = \sum_{y \in \mathcal{E}} U_{wall,y} \cdot F_{wall,y} \cdot \left(T_{out} - T_{in,z}\right) \quad (69)$$

$$\dot{Q}_{win,z} = \sum_{y \in \mathcal{E}} U_{win,y} \cdot F_{win,y} \cdot \left(T_{out} - T_{in,z}\right) \quad (70)$$

$$\dot{Q}_{sw,z} = \sum_{y \in \mathcal{E}} a_w \cdot R_{se} \cdot U_{wall,y} \cdot F_{wall,y} \cdot I_{T,z} \quad (71)$$

$$\dot{Q}_{sg,z} = \sum_{y \in \mathcal{E}} \tau_{win} \cdot SC \cdot F_{win,y} \cdot I_{T,z} \quad (72)$$

$$\dot{Q}_{in,wall,z} = \textstyle\sum_{y \in \mathcal{E}} U_{wall,y} \cdot F_{wall,y} \cdot \left(T_{in,nz} - T_{in,z}\right) \quad (73)$$

By appropriately modifying (68) -(73), the state space system of equations is obtained for each building.

$$\frac{d\boldsymbol{T_{in}}(t)}{dt} = \boldsymbol{A_b} \cdot \boldsymbol{T_{in}}(t) + \boldsymbol{B_b} \cdot \boldsymbol{U} \quad (74)$$

$$\boldsymbol{Y}(t) = \boldsymbol{C_b} \cdot \boldsymbol{T_{in}}(t) + \boldsymbol{D_b} \cdot \boldsymbol{U} \quad (75)$$

The system of continuous time equations (74) -(75) is converted to discrete time equations (76) -(77).

$$\boldsymbol{T_{in}}(k+1) = \boldsymbol{A_{b,d}} \cdot \boldsymbol{T_{in}}(k) + \boldsymbol{B_{b,d}} \cdot \boldsymbol{U} \quad (76)$$

$$\boldsymbol{Y}(k) = \boldsymbol{C_{b,d}} \cdot \boldsymbol{T_{in}}(k) + \boldsymbol{D_{b,d}} \cdot \boldsymbol{U} \quad (77)$$

2.6 Building Energy System Modeling

An energy storage unit is presented in this section. Let us assume that the optimal active power of the battery is $P_{bat}(t)$ and load convention is used then the SoC (in kWh) of the battery, SoC_{bat}, is calculated according to the following equation.

$$SoC_{bat}(t+\Delta t) = \begin{cases} SoC_{bat}(t) + P_{bat}(t) \cdot n_{ch} \cdot \Delta t, & P_{bat}(t) \geq 0 \\ SoC_{bat}(t) + \dfrac{P_{bat}(t)}{n_{disch}} \cdot \Delta t, & P_{bat}(t) < 0 \end{cases} \quad (78)$$

where n_{ch}, n_{disch} are the charging and discharging efficiency coefficients of the battery.

Chapter 3

3. Optimal operation scheduling of the CCHP system

3.1 PSO algorithm

In this work, particle swarm optimization (PSO) has been used in order to optimally schedule the operation of the examined system. PSO is one of the most highly efficient heuristic methods and its implementation is remarkably simple. PSO has proved very robust and efficient for application to complex optimization problems as it does not depend on the selected initial point and leads to a global optimum with a high rate of success. It is difficult to find the global optimum for large-dimension optimization problems and formulate extremely complex objective functions using classical methods.

In the examined problem, the building thermal model's differential equations should be solved within the optimization procedure, making its formulation difficult if classical optimization techniques are applied. However, using PSO algorithm, this problem does not appear since the building thermal model, regardless of its complexity, can be included in the objective function.

3.2 Augmented Objective function

The objective of the PSO algorithm is to minimize the total daily operation cost of the examined system on the assumption of operation under variable electricity and natural gas prices. It determines the temperature of the working fluid of the engine (T_h), the Usage Factor Coefficient (uf) representing the percentage of thermal energy that will be provided for cooling and hot water, the optimal active power of the energy storage system (P_{bat}) and the coefficient representing the exploitation percentage of the thermal energy for hot water (hw_c), within a predefined optimization period. To this end, it schedules optimally the total building's thermal power for cooling and hot water. At the same time, a large number of constraints including all the operational and technical constraints of Stirling engines and the building energy systems are satisfied e.g., an acceptable thermal comfort for the occupants of each thermal zone of the building should be maintained and a proper amount of electric power should be provided for the electrical loads.

The augmented cost function used by the PSO including the applied constraints, is given in (79). The algorithm aims to minimize the total operational cost of the grid-connected CCHP system while satisfying all of the associated technical and operation constraints integrated in term (Pen) of the objective function and they are analyzed in Section 3.3.

$$\mathrm{TC} = \min_{\substack{T_h, uf, P_{bat}, \\ hw\_c}} \left\{ \left(\sum_t P_{grid}(t) \cdot EP(t) + \sum_t M_{FF}(t) \cdot FP \right) \cdot \Delta t + Pen \right\} \tag{79}$$

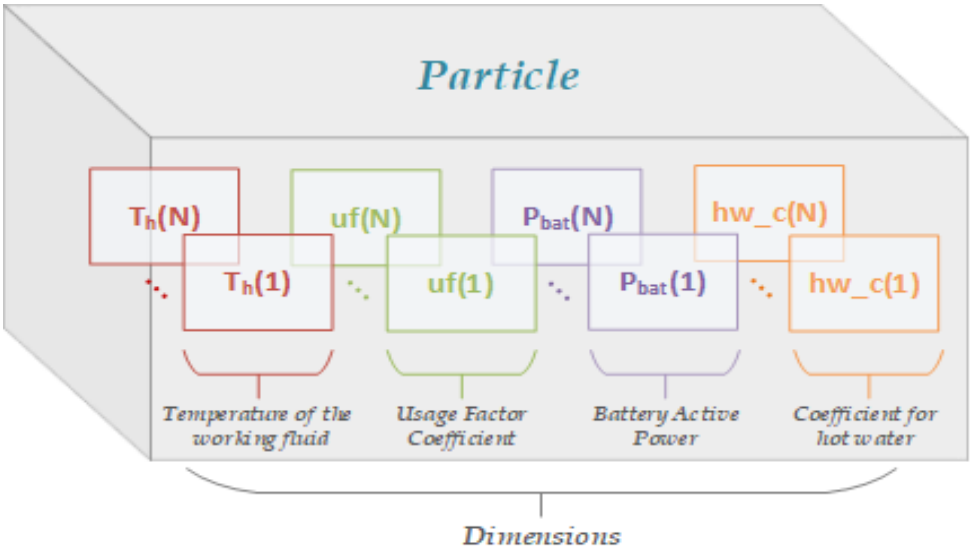

Fig. 13 Particle structure of the examined problem

3.3 Constraints and Power dispatch

3.3.1 Sub-optimization problem

Sub-optimization problem is solved in order to optimally dispatch the total thermal power of each building to its thermal zone. The estimated indoor temperature of a thermal zone is used with its upper and lower limits to suitably define the flexibility of each building thermal zone to increase or decrease its thermal power demand as in the following equations. [21]

$$FL_z^{\uparrow}(t) = \frac{T_{in,z}(t) - T_{min,z}}{T_{max,z} - T_{min,z}} \tag{80}$$

$$FL_z^{\downarrow}(t) = \frac{T_{max,z} - T_{in,z}(t)}{T_{max,z} - T_{min,z}} \tag{81}$$

The total thermal power of a building ($Q_{ev,total}$) to its thermal zones is optimally dispatched according to the following equation.

$$Q_{ev,z}(t) = \frac{FL_z(t) \cdot V_z}{\sum_z \{FL_z(t) \cdot V_z\}} \cdot Q_{ev,total}(t) \tag{82}$$

3.3.2 Constraints

- *Building Thermal Load Constraints*

$$Q_{ev,total,min} \leq Q_{ev,total}(t) \leq Q_{ev,total,max} \tag{83}$$

$$Q_{ev,z,min} \leq Q_{ev,z}(t) \leq Q_{ev,z,max} \quad (84)$$

$$\sum_{z} Q_{ev,z}(t) = Q_{ev,total}(t) \quad (85)$$

$$T_{min,z} \leq T_{in,z}(t) \leq T_{max,z} \quad (86)$$

- *Battery Constraints*

$$SoC_{bat,min}(t) \leq SoC_{bat}(t) \leq SoC_{bat,max}(t) \quad (87)$$

$$P_{bat,min}(t) \leq P_{bat}(t) \leq P_{bat,max}(t) \quad (88)$$

$$SoC_{bat}(T_0) = SoC_{bat}(T_f) \quad (89)$$

- *Heater Constraints*

$$T_{min,h} \leq T_h(t) \leq T_{max,h} \quad (90)$$

- *Storage Tank Constraints*

$$SW_{min} \leq SW(t) \leq SW_{max} \quad (91)$$

$$SW(T_0) = SW(T_f) \quad (92)$$

- *Network Constraints*

Let us consider that the state of operation of the examined system is denoted with the variable st_{grid} and the system operates autonomously for $t \in [T_{auto,0}\ T_{auto,f}]$.

$$st_{grid}(t) \cdot P_{grid,min} \leq P_{grid}(t) \leq st_{grid}(t) \cdot P_{grid,max} \quad (93)$$

$$P_{el,b}(t) + P_{bat}(t) = st_{grid}(t) \cdot P_{grid}(t) \quad (94)$$

with,

$$st_{grid}(t) = \begin{cases} 0, & \forall t \in [T_{auto,0}\ T_{auto,f}] \\ 1, & otherwise \end{cases} \quad (95)$$

3.4 Algorithm Overview

The energy management flowchart of the proposed grid-connected CCHP system is shown in Figure 14. Initially, the daily forecasts are received for the next 24-hour period. Once the forecast data is available, the models presented in the previous section are executed. Then, system operation is optimally scheduled to minimize eq. (79).

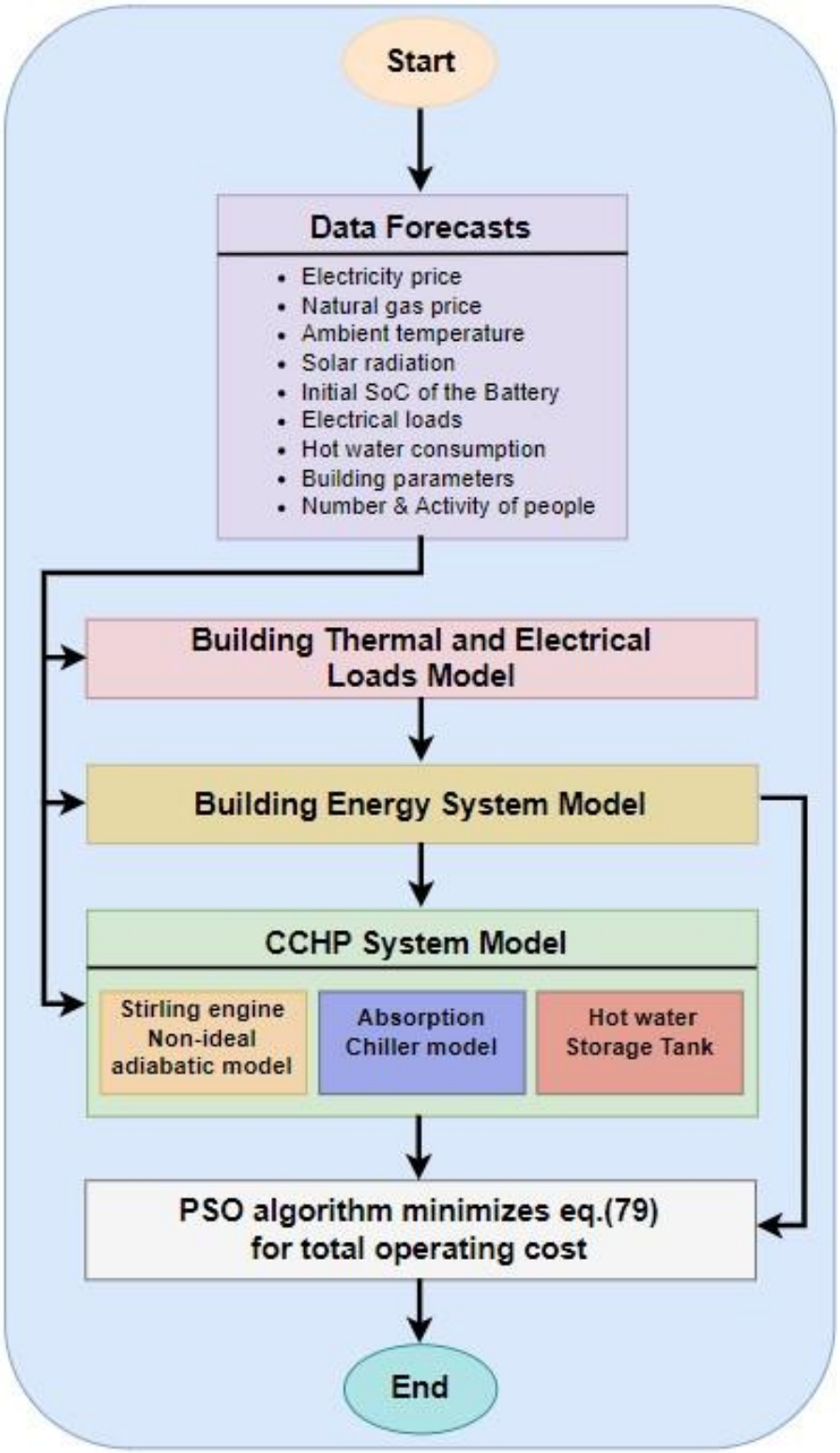

Fig. 14 System Energy Management Flowchart

Chapter 4

4. Case study – Results

The developed CCHP system is verified through the simulation of 2 operating scenarios. This section presents a 24-hour case study under which the system is being examined. Input data parameters for this case study are given below. However, considering the above thermal load model, a wide variety of case studies can be examined just by properly adjusting building's thermal zones number, size, floor plan and construction characteristics. In this way, system behavior is investigated under realistic operating conditions. The optimization algorithm described above contributes to find the optimal operation strategy of the system in order to minimize operating cost. The results of the examined scenarios are also presented and discussed.

4.1 Case study

The geometrical and operational characteristics used to model the prime mover of the proposed system are derived from the GPU-3 engine specifications and are given in Table 3 and Table 4, respectively. Hence, non-ideal adiabatic analysis is performed.

GPU-3	***Engine specifications***
Cylinder bore at liner	6.99 cc
Cylinder bore above liner	7.01 cc
Cooler	
Tube length	4.61 cm
Heat transfer length	3.55 cm
Tube inside diameter	0.108 cm
Tube outside diameter	0.159 cm
Number of tubes per cylinder (or per regenerator)	312 (312/8 = 39)
Void volume	13.8 cc
Heater	
Heat transfer length	15.54 cm
Cylinder tube	11.64 cm
Regenerator tube	12.89 cm
Mean tube length	11.64+12.89 = 24.53 cm
Tube inside diameter	0.302 cm
Tube outside diameter	0.483 cm
Number of tubes per cylinder (or per regenerator)	40 (40/8 = 5)
Void volume	70.28 cc

Cold end connecting tubes	
Length	1.59 cm
Duct inside diameter	0.597 cm
Number of ducts per cylinder	8
Cooler end cap	0.279 cc
Regenerator	
Length	2.26 cm
Inside diameter	2.26 cm
Number per cylinder	8
Material	Stainless steel wire cloth
Number of wires per cm	79x79
Wire diameter	0.004
Number of layers	308
Filler factor (%)	30.5
Void volume	50.55 cc
Drive mechanism	
Connecting rod length	4.60 cm
Crank radius	1.38 cm
Eccentricity	2.08 cm
Miscellaneous	
Displacer rod diameter	0.952 cm
Piston rod diameter	2.22 cm
Displacer diameter	6.96 cm
Piston diameter	6.99 cm
Displacer length	4.35 cm
Displacer wall thickness	0.159 cm
Displacer stroke	3.12 cm
Expansion space clearance	0.163 cm
Compression space clearance	0.030 cm
Buffer space maximum volume	521 cc
Working space minimum volume	233.5 cc
Clearance around hot cap	0.025 cm
Clearance volumes	
Compression space	28.68 cc
Expansion space	30.52 cc
Swept volumes	
Compression space	114.13 cc
Expansion space	120.82 cc

Table 3 GPU-3 engine dimensions and specifications.

General Motors Corporation designed this external combustion engine with built-in generator for electrical power supply. The GPU-3 is a B-type configuration Stirling engine. The displacer and the power piston are located in the same cylinder driven by a rhombic drive mechanism. A view of the engine with all of its components is shown in Figure 15. However, the power generated from the GPU-3 Stirling engine is not sufficient for the examined case study, because of its size. For this reason, and considering the thermal loads as estimated from the thermal load model, 3 of these engines with similar specifications, are used to compose the proposed system.

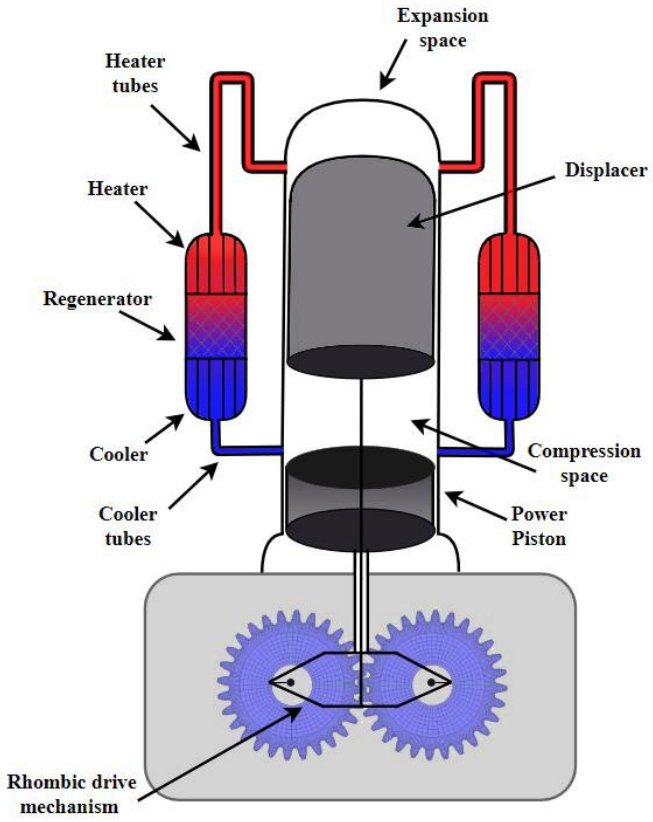

Fig. 15 GPU-3 Striling Engine B-type

	Operational engine parameters
Engine configuration	B-type
Drive mechanism	Rhombic
Working fluid	Helium (He)
Total mass of working fluid	1.1362 gr
Wall temperature of heater	877-977 K
Wall temperature of cooler	373 K
Mean engine pressure	4.13 MPa
Engine frequency	41.72 Hz

Table 4 GPU-3 operational parameters.

In this case study, a summer scenario is considered, and the absorption chiller is therefore used to provide chilled water for cooling applications. Design parameters considered for the thermodynamic analysis of the refrigeration system are listed in Table 5.

Parameter	*Symbol*	*Value*
Evaporator temperature	T_{10}	6 °C
Generator temperature	T_4	90 °C
Maximum capacity of generator	Qg	28.3 kW
Heat exchanger efficiency	Eff_{HX}	0.53
Weak solution mass fraction	X_1	57% LiBr
Strong solution mass fraction	X_4	62% LiBr

Table 5 Absorption chiller design parameters.

The system prime mover comprises 3 Striling engines with the same characteristics as described above. The overall amount of waste heat is provided for cooling and hot water through the use of an absorption chiller and a hot water storage tank, respectively. Furthermore, the system is connected to the main power grid for power exchange during operation. In particular, additional power is supplied from the main grid when electricity demand peaks. Otherwise, the system sells power to the main grid. This results in a further reduction in operating costs. A scenario with an integrated energy storage unit is also investigated in case the examined system operates autonomously. The proposed CCHP system with all external integrations is shown in Figure 16.

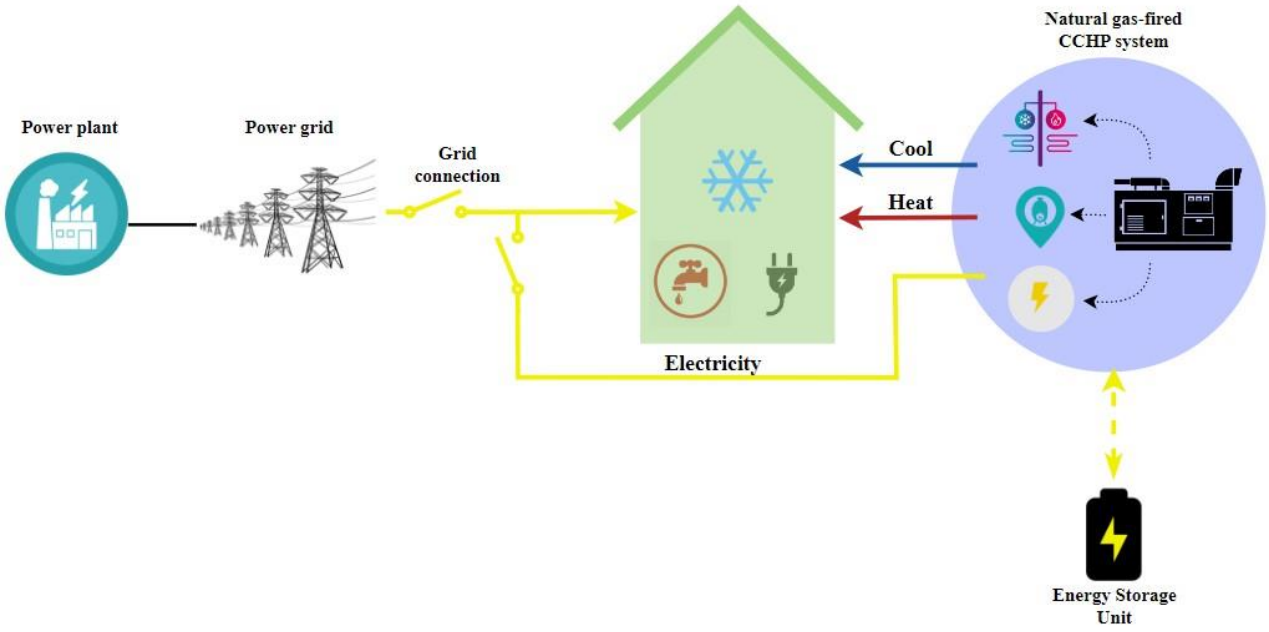

Fig. 16 The proposed CCHP system

The suggested approach was applied to a residential building consisting of 2 floors and 12 thermal zones. Table 6 includes the necessary building's model parameter data. Building floor plan determines the borders and parameters of every thermal zone. Therefore, contributes to dispatch the total thermal energy and allows independent control of zones temperatures. The required thermal energy of each zone is evaluated from building's thermal model considering several parameters such as absorbance coefficient of an external wall, window's glass transmission coefficient and others attributes contained in Table 6. Two similar floors, as shown in Figure 17, each consisting of 6 thermal zones, were selected for demonstration purposes.

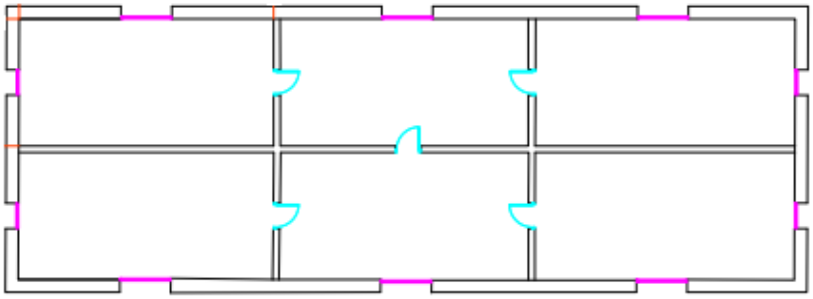

Fig. 17 Floor plan of the building.

THERMAL ZONES MODELING DATA							
Building thermal zones specifications							
Side_1 (m)	7	$\boldsymbol{p_z(kg/m^3)}$	1.2	$\boldsymbol{\tau_{win,z}}$	$1.1 \cdot 10^{-3}$	$\boldsymbol{\beta_z}(°)$	90
Side_2 (m)	9	$\boldsymbol{C_z(kWh/(kg \cdot °C))}$	1/3600	$\boldsymbol{a_{w,z}}$	$18.6 \cdot 10^{-3}$	$\boldsymbol{\theta}(°)$	11.9
Height (m)	3.5	$\boldsymbol{U_{wall,z}(kW/(m^2 \cdot °C))}$	$2.04 \cdot 10^{-3}$	$\boldsymbol{SC_z}$	0.54	$\boldsymbol{\theta_z}(°)$	39.9
Tmin / Tmax (°C)	20/25	$\boldsymbol{U_{win,z}(kW/(m^2 \cdot °C))}$	$5.6 \cdot 10^{-3}$	$\boldsymbol{p_g}$	0.2	$\boldsymbol{R_{se,z}((m^2 \cdot °C)/kW)}$	40
BUILDING PARAMETERS							
Number of floors					2		
Total number of thermal zones					12		

Table 6 Building and Thermal zones parameters

A typical time series of hot water consumption in residential buildings over a 24-hour period is shown in Figure 18. Based on the consumption of hot water appears to have a residential building, the storage tank capacity is selected. The reference temperature at which the hot water is supplied is set at around $60\ °C$, as in most heating systems. The temperature of the incoming water to be heated is not deterministic. Hence, for demonstration purposes, it is assumed to be $15\ °C$, which is typically a good approximation. Table 7 is a summary of all the above heating system operating parameters.

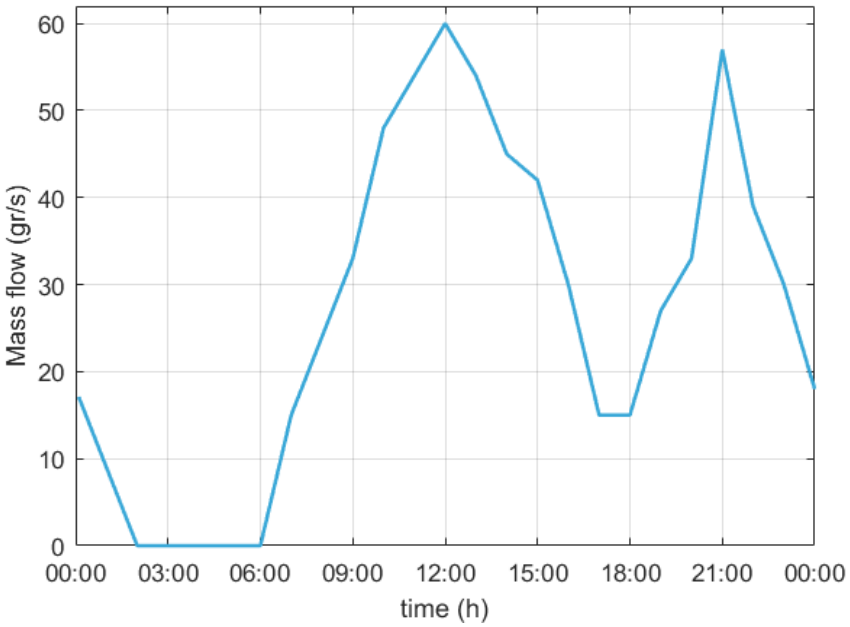

Fig. 18 Mass flow consumption of hot water

Parameter	*Value*
Tank Capacity	1500 L
T_{ref}	*60 ° C*
T_{urb}	15 °C

Table 7 Hot water storage tank parameters

The ambient temperature that was used in this case study is shown in Figure 19 and it is a typical daily temperature time series from late summer in Greece.

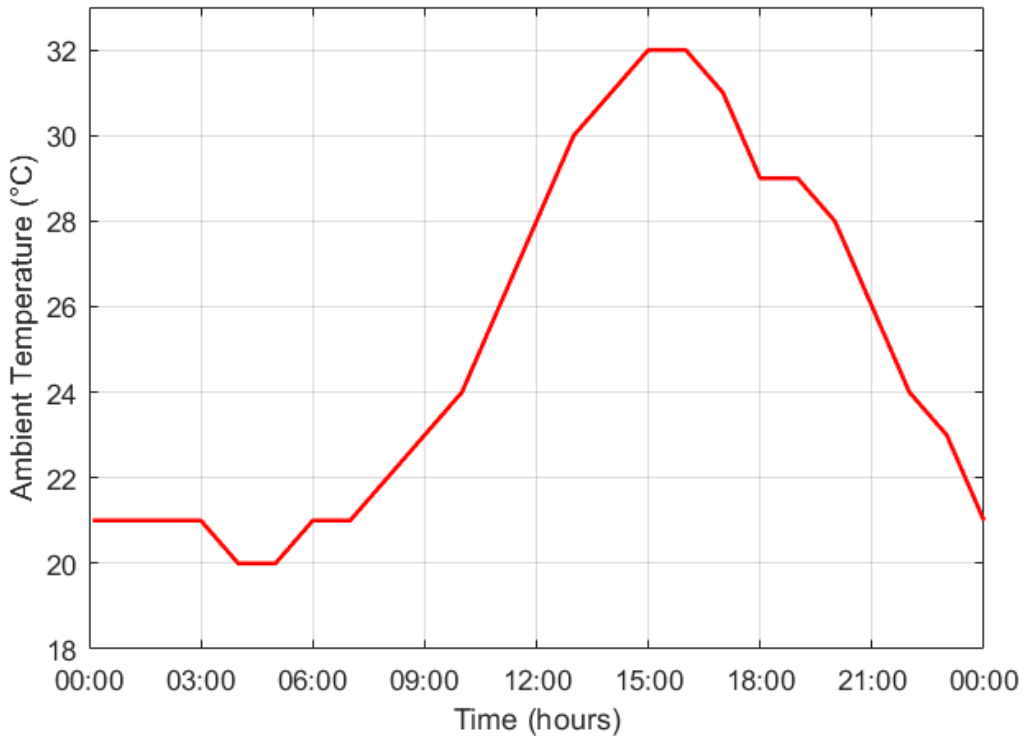

Fig. 19 Ambient temperature during a 24-hour period.

The time series of the electricity price forecast that was used in the examined scenario is given in Figure 20. It was assumed that the electricity price that was forecasted was carried out by the power system operator and provided to the building. Provided that the computation time that is required by the proposed method is small, it was assumed that the electricity price forecast would be provided to the local electricity market participants after the day-ahead electricity market was carried out.

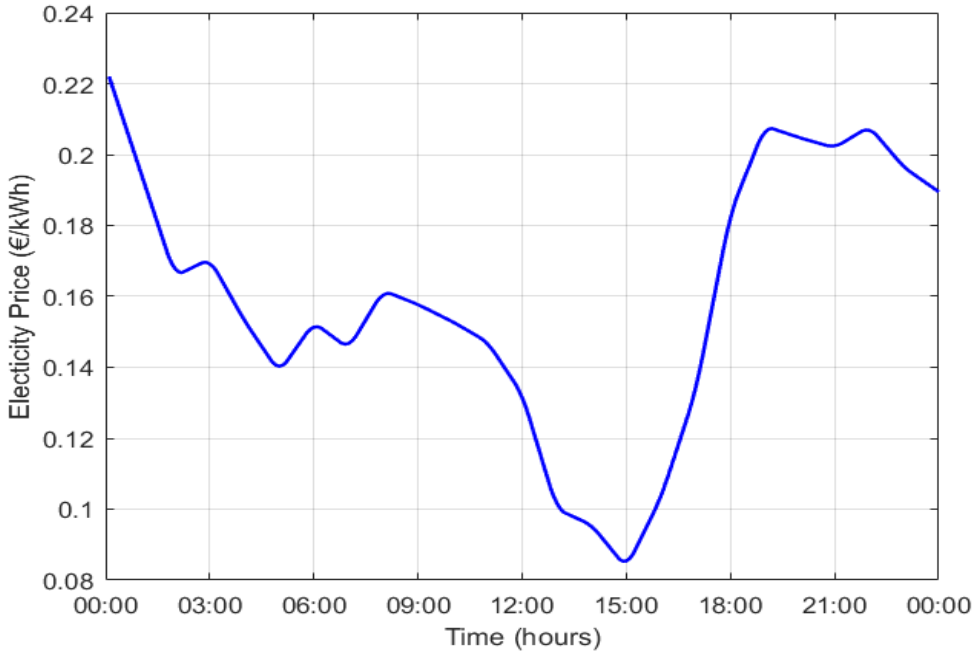

Fig. 20 Forecasted electricity price during a 24-hour period.

As already mentioned, one of the benefits of using a Stirling engine as system's prime mover is the fuel flexibility, since it is an external combustion engine. This means that a range of fuels can be used to power the CCHP system, combined with a compatible combustion system. In the case study being examined, natural gas has been selected as systems' heat source. This type of fossil fuel provides several benefits that make it an enticing choice. First and foremost, it results in lower pollutant emissions compared to other fossil fuels, such as coal or petrol, to provide the same amount of energy. In addition, considering that most European countries have an established distribution network that delivers natural gas incessantly, domestic availability is assured. Finally, at the time of this writing, natural gas offers a relatively lower cost than other fossil fuels. In this way, a further reduction in the operating costs of the system is achieved.

Natural gas price is set on a monthly basis on the energy market and is offered through bilateral contracts between the consumer and the supplier. The graph below shows the price of natural gas for the past months in Greece, as extracted from the "Regulatory Authority for Energy" company. This price is established on the basis of the data provided to the company. For the purpose of examining the system, the most recent available price, as shown in the following figure, was used as the natural gas price. Additional commission and shipping fees are also included in the final cost.

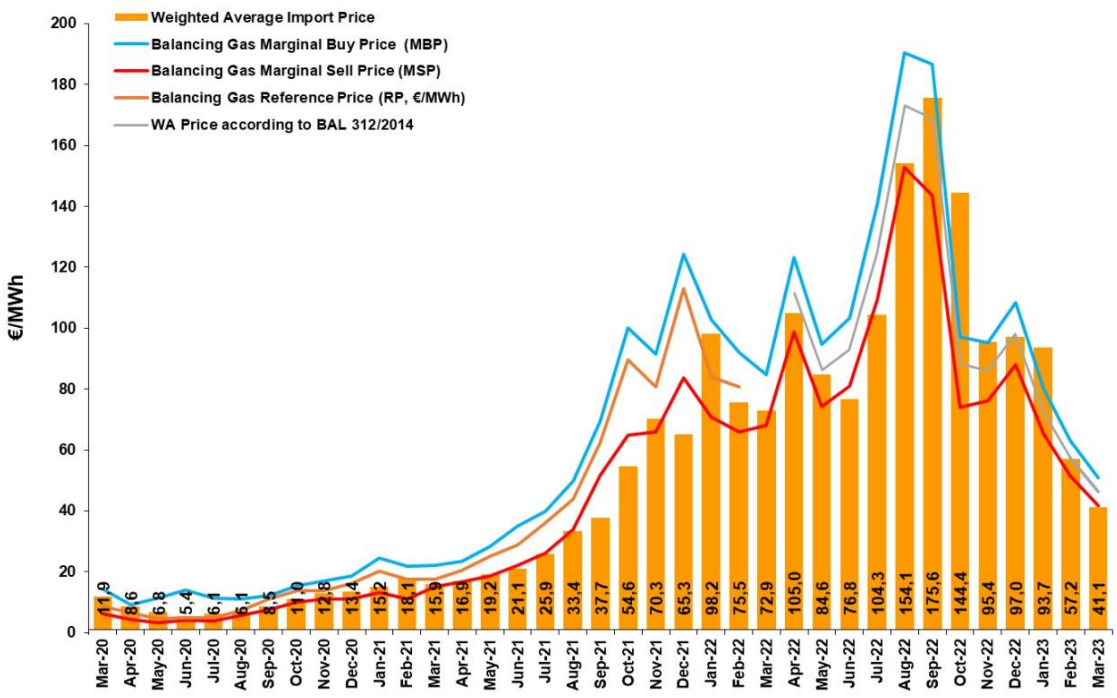

Fig. 21 Natural gas price as extracted from "Regulatory Authority for Energy" company

The electrical power consumption of each building thermal zone is given in Figure 22a. The modeling of the energy consumption profiles in residential thermal zones was developed taking into consideration the number, age and the activity level of the occupants as well as the number, type, and the usage of electric household appliances [22], [23]. The total electric power consumption of the examined building is depicted in Figure 22b.

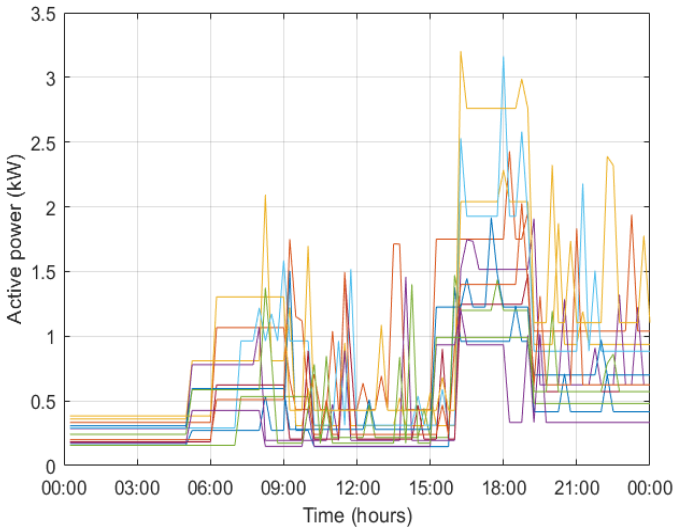

Fig.22a Forecasted electric power consumption of each thermal zone

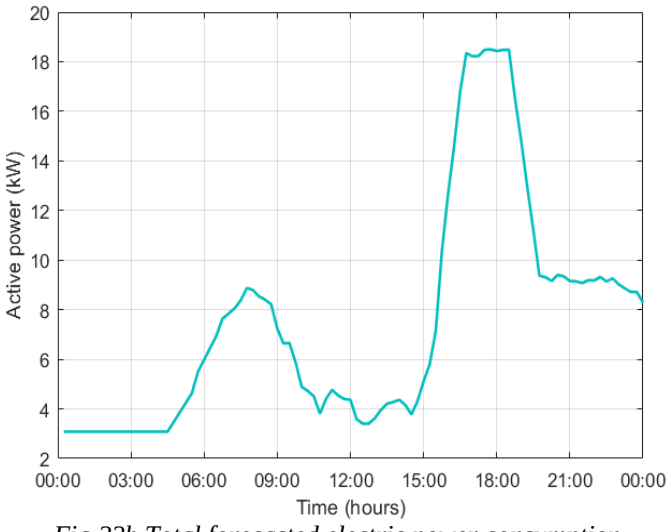

Fig.22b Total forecasted electric power consumption

Technical characteristics of the integrated battery used for the electrical loads in this case study are shown in Table 8.

BATTERY TECHNICAL CHARACTERISTICS

$\boldsymbol{Battery\ Capacity\ (kWh)}$	60
$\boldsymbol{SoC_{max}\ /SoC_{min}\ (kWh)}$	54/6
$\boldsymbol{P_{max}\ /P_{min}}$ **(kW)**	12/-12

Table 8

4.2 Results

With the purpose of examining the proposed CCHP system, 2 different operating scenarios were considered for a 24-hour time period, and therefore their operational behavior is carried out. The results for each of the scenarios considered are presented and discussed in the following subsections.

The thermodynamic analysis of the absorption chiller is performed considering the nominal design parameters given in the case study. In this manner, the thermodynamic analysis calculates the enthalpy, mass flow rate, pressure, temperature and concentration of LiBr for every absorption cycle point. The obtained results are presented in Table 9.

$\boldsymbol{Point}$	$\boldsymbol{h\ (kJ/kg)}$	$\boldsymbol{\dot{m}\ (kg/s)}$	$\boldsymbol{p\ (kPa)}$	$\boldsymbol{T\ (°C)}$	$\boldsymbol{X\ (\%\ LiBr)}$	$\boldsymbol{Remarks}$
1	104.03	0.1137	0.94	40	57.6	
2	104.03	0.1137	7.38	40	57.6	
3	162.13	0.1137	7.38	66.5	57.6	Sub-cooled liquid
4	222.92	0.1048	7.38	90	62.4	
5	159.91	0.1048	7.38	63.5	62.4	
6	159.91	0.1048	0.94	49.7	62.4	
7	2647.9	0.0089	7.38	79	0	Steam
8	167.54	0.0089	7.38	40	0	Saturated liquid
9	167.54	0.0089	0.94	6	0	
10	2511.9	0.0089	0.94	6	0	Saturated vapor

Table 9 Results obtained from the chiller's thermodynamic analysis

4.2.1 Scenario I

The operation of the grid-connected CCHP system aims to meet the thermal and electrical loads during a 24-hour period at the lowest possible cost. The thermal energy required for cooling and heating, as well as the electricity demand, are shown in the results below. The results obtained are based on the forecasted input variables mentioned in the case study above.

The internal temperature for each building thermal zone for scenario I, is shown in Figure 23. Upper and lower temperature limits are also presented ($i.e.\ 20\ °C - \ 25\ °C$). It is observed that the internal temperature of all of the thermal zones range between the upper and lower limits of the comfortable temperature. There is also a tendency for their temperature fluctuations to have the same behavior with each other. Additionally, internal temperatures are proportional to ambient temperature. In this manner, they are getting closer to the lower (upper) temperature limit for the period of time where the ambient temperature is minimum (maximum).

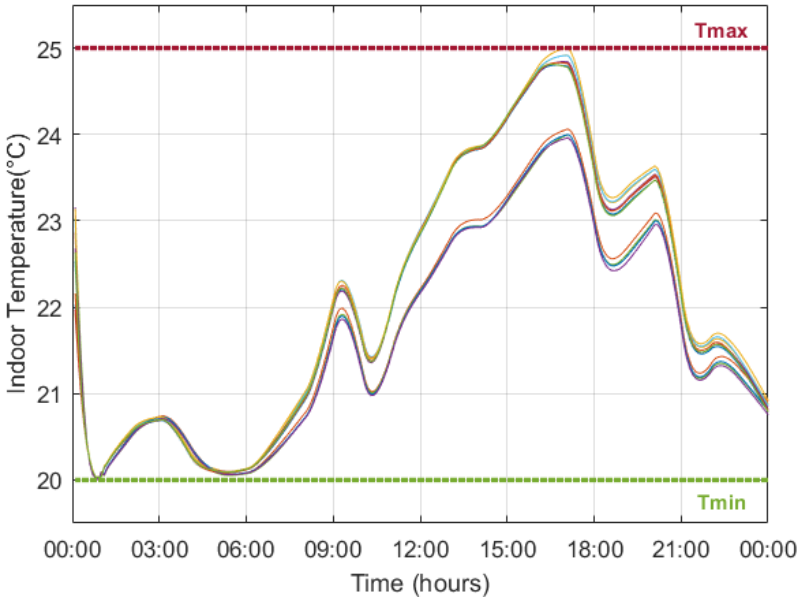

Fig. 23 Thermal zones indoor temperature, Scenario I

The total cooling power consumption for the specific building is presented in Figure 24a. It results from the execution of the building thermal loads model with consideration of the forecasted input parameters provided in the case study. In this way, the indoor temperatures remain within the comfortable temperature range as shown above. The total cooling power follows the ambient temperature, and thus higher cooling power demand is observed for periods of time where ambient temperature peaks (e.g. 15:00). The flexibility coefficient is used for each thermal zone and contributes to the optimal dispatch of the cooling power provided by the absorption chiller. The prevailing temperature and the structure characteristics of each thermal zone, are some of the parameters which have an impact on the power dispatch. In any case, as shown in Figure 24b, the cooling power is proportional to the outdoor temperature. However, it is observed that, according to building structure, the thermal zones consisting of 2 external walls instead of 1 are more affected by the ambient temperature variations.

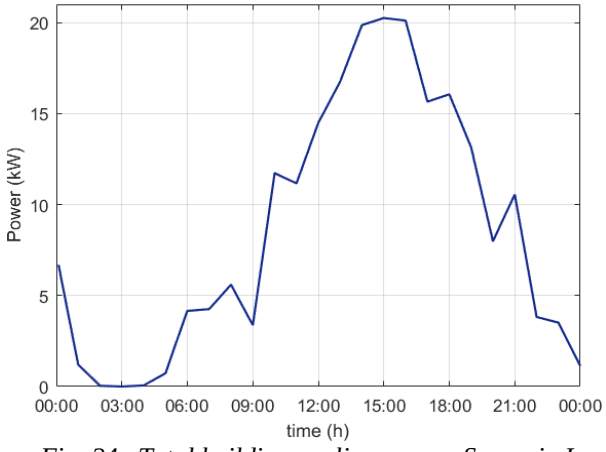

Fig. 24a Total building cooling power, Scenario I

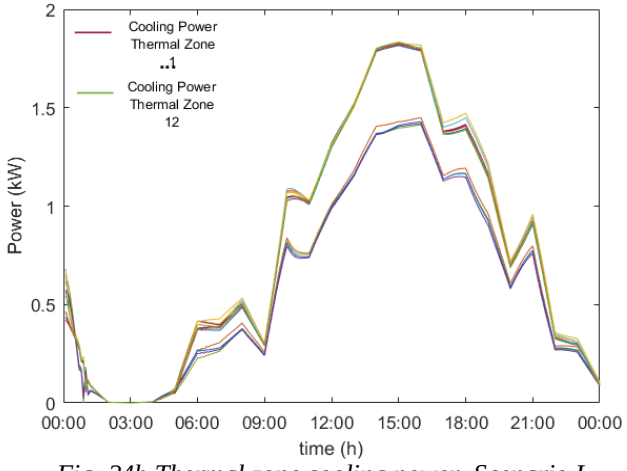

Fig. 24b Thermal zone cooling power, Scenario I

The total power exchanged with the main electric grid over a 24-hour period of time is shown in Figure 25. The minus or plus sign of the active power indicates the power flowing from the CCHP system to the grid and vice versa, respectively. The power flow depends on several parameters such as electricity price and electrical power consumption of the building. It is observed that there is a steep increase in power consumption from 15:00 to 20:00. However, the CCHP system cannot provide all the electricity needed. As a result, a percentage of the total power demand is supplied by the main grid during this period. In all other cases, the system follows the building's cooling demand. Any excess electric power is sold to the grid.

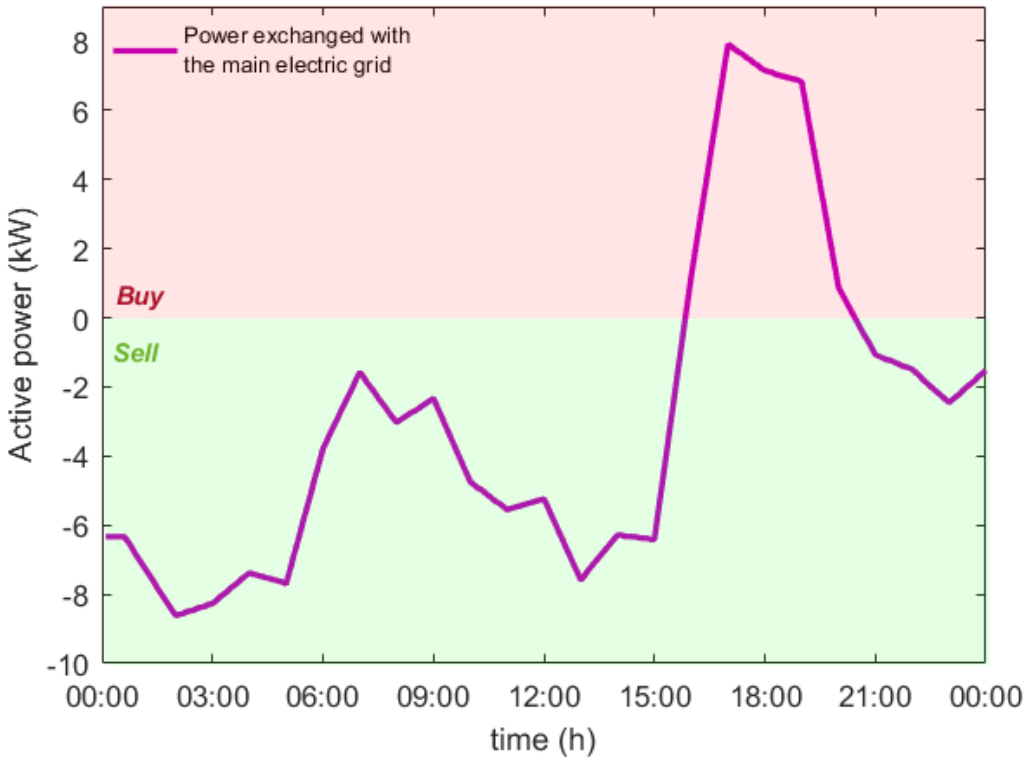

Fig. 25 Active Power Flow, Scenario I

Waste heat is provided for heating applications through the use of eq. (61). During periods of low cooling demand, a large amount of waste heat is provided for hot water. This is due to the "Following Thermal Load" operating strategy. It is observed that during the night hours, when the demand for cooling is low, a significant amount of thermal energy is provided for hot water. In addition, during the same hours, hot water consumption is zero for most of the time. This has created the need for a coefficient that determines the percentage of the available heat that is being utilized, i.e. *hw_c* coefficient. On the other hand, more cooling demand is needed as the hours go by, so the amount of thermal energy available for hot water is limited during the day. Therefore, choosing the right tank capacity is required to store enough hot water to meet the daily needs of the building. Figure 26 shows all of the above mentioned.

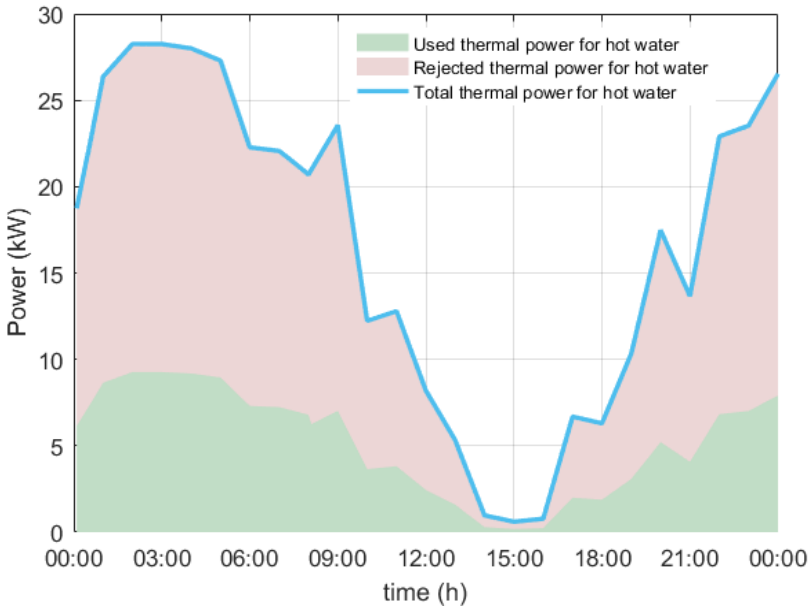

Fig. 26 Hot water thermal power, Scenario I

In the scenario being examined, the water storage tank is nearly empty at the beginning of the day, as shown in Figure 27. In this way, it utilizes as much energy as possible during the night hours instead of wasting it. Neither the cooling demand nor the hot water consumption is sufficient at that time. Therefore, the stored water volume is near the upper capacity limit. As soon as the hot water starts to flow, the tank continues to fill up, but at a reduced rate (6:00 – 9:00 a.m.). At around 9 a.m., there is a gradual increase in cooling demand as the ambient temperature rises. This results in a reduction in the thermal energy provided for hot water. Consequently, the amount of hot water outflow is greater than the inflow. The storage tank capacity has been properly selected so as to meet the daily hot water demand.

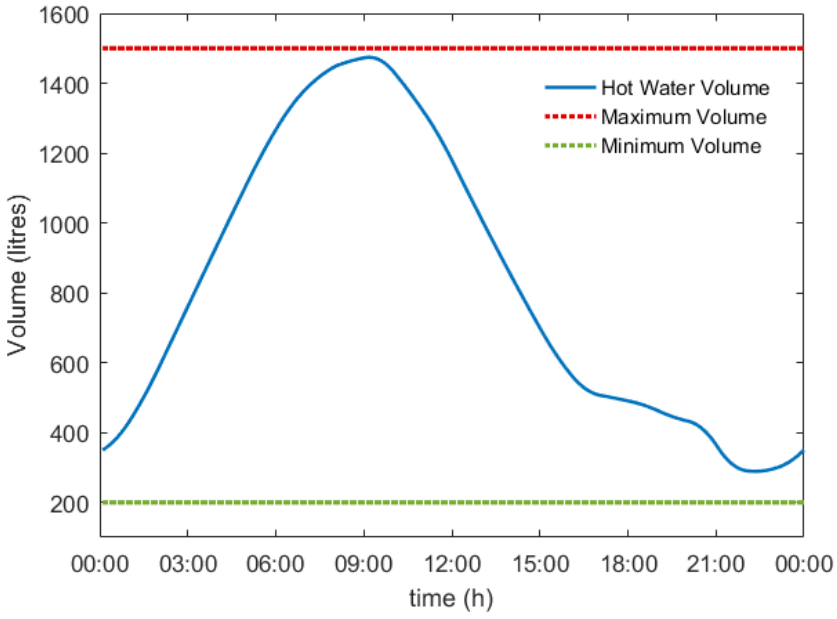

Fig. 27 Hot water volume, Scenario I

PSO algorithm determines the optimal system operation for the case study under consideration as shown in Figure 28. In conjunction with the selected operating strategy, i.e. "Following thermal load", the uf factor provides the thermal energy required for cooling purposes with respect to the ambient temperature fluctuations. In this way, the indoor temperatures shown above are well maintained within the temperature limits. In addition, to meet electrical loads and achieve optimal operation, the power generated by the system is properly managed as already described.

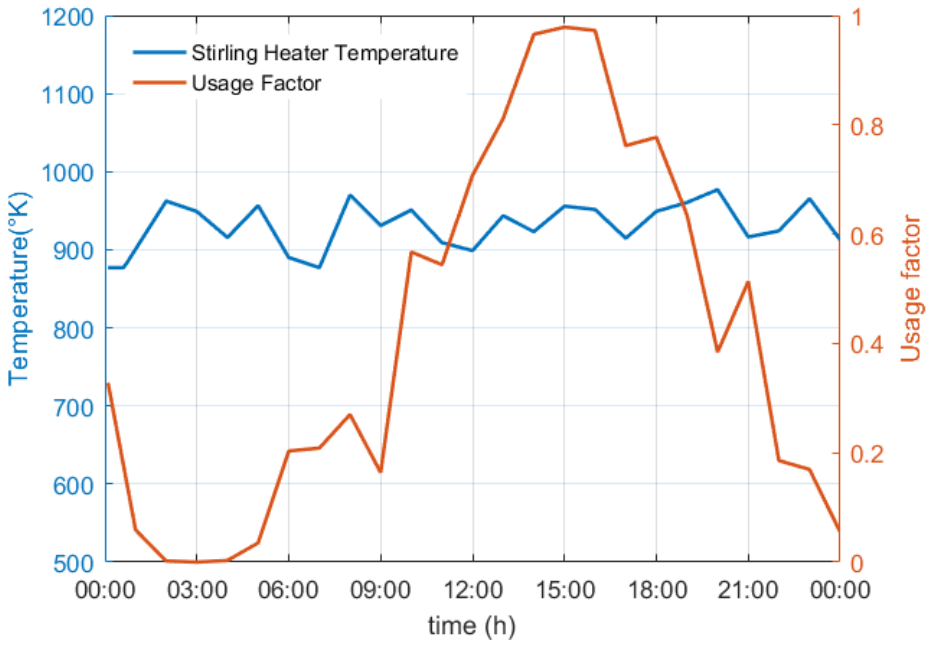

Fig. 28 PSO decision variables, Scenario I

All constraints are maintained in the scheduling of the above operational scenario. Optimal operating cost is also achieved. The total system operation cost obtained for Scenario I is 7.887 $(m.u.)$.

4.2.2 Scenario II

In the second scenario, the CCHP system is examined with an integrated energy storage unit. This gives the system an additional option off the grid to supply the excess electrical loads that the CCHP system cannot cover. In this way, the system has the ability to operate autonomously for a period of time. Therefore, system disconnection from the grid is examined for 2 hours. The purpose of this scenario is to test the system's response to these changes. This scenario is compared to the one previously mentioned. The differences in a 24-hour period caused by autonomous operation and battery integration are discussed.

In this scenario, indoor temperatures behave similar to those seen in scenario I. They are proportional to the ambient temperature fluctuations. In this way, thermal zone temperatures reach

their maximum (minimum) value when the ambient temperature is at its maximum (minimum). Furthermore, the upper and lower limits of the comfortable temperature remain unchanged. However, as shown in Figure 29, there are some notable differences. More specifically, it can be observed that the indoor temperatures over the 24-hour period are in a lower range than those previously presented. They also appear to be more resistant to changes in ambient temperature and have less vibration. This is due to the integrated battery, which recharges during periods of low power and cooling demand. In this way, the waste heat that is generated during the battery charging process is evenly distributed throughout the day for cooling purposes. Therefore, it can be concluded that the battery contributes to a better regulation of the temperatures in the thermal zones.

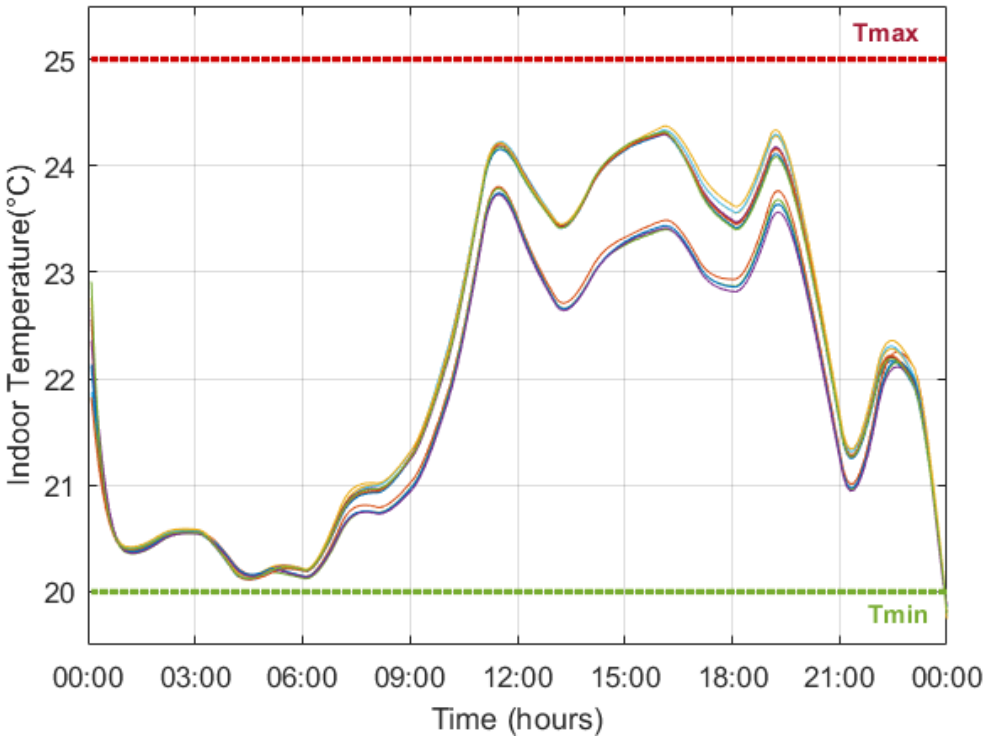

Fig. 29 Thermal zones indoor temperature, Scenario II

Total building cooling power depends on parameters mentioned previously. Although, battery charge is now another parameter to consider. In Figure 30a, it is observed that even during some periods of low cooling demand, the amount of thermal energy supplied for cooling purposes is higher in this scenario, e.g. at 8:00 am. This is due to battery recharging during periods of low power and cooling demand. As a result, the CCHP system dissipates a greater amount of waste heat, which in turn is provided to the thermal zones, as indicated in Figure 30b. In this way, the temperature profile of the thermal zones is formed as shown in the figure above. However, this operating strategy reduces cooling power during periods of high demand. For example, it is noted that the period of time during which the cooling power is greater than 15 kW is reduced by 1.5 hours, $i.e. 12{:}00 - 18{:}30 \rightarrow 12{:}30 - 17{:}30$.

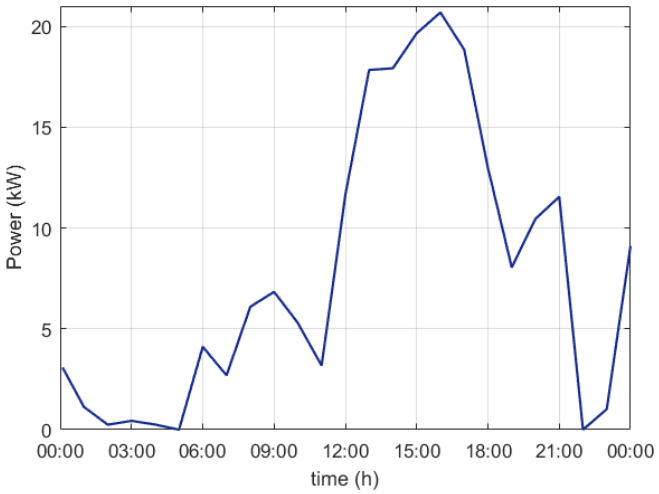

Fig. 30a Total building cooling power, Scenario II

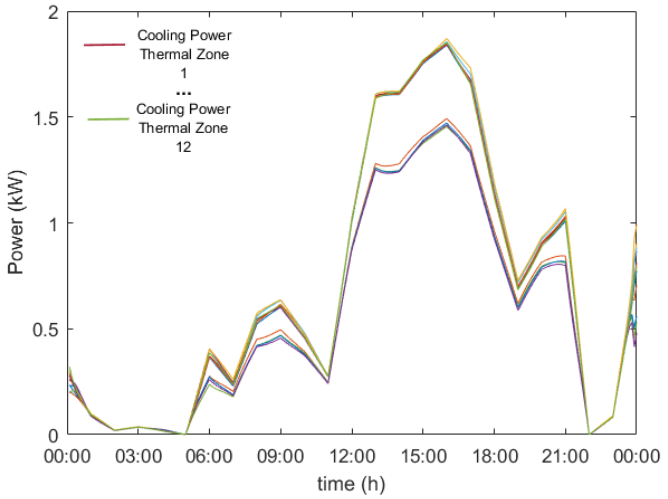

Fig. 30b Thermal zones building cooling power, Scenario II

The total power exchanged with the main electric grid in autonomous operation is shown in Figure 31. In this scenario an autonomous operation of the CCHP system from 15:00 to 17:00 is examined. During this time, neither the system nor the grid can sell power to each other. Therefore, all electrical power is supplied by both the system and the battery. Battery integration has brought several changes to the way the system interacts with the grid. More specifically, it is observed that during periods of low electrical demand, less energy is injected into the main grid. This is a result of the battery charging at that time. On the other hand, when high electrical demand is observed, the battery also reduces the power that is supplied by the main grid. Consequently, it is well understood that the battery enhances the autonomous operation of the system. In addition, the battery provides the system with an additional option for covering the excess electrical loads. This allows the optimization algorithm to adjust and optimally schedule the times when the system exchanges power with the grid. Thus, cost minimization is achieved.

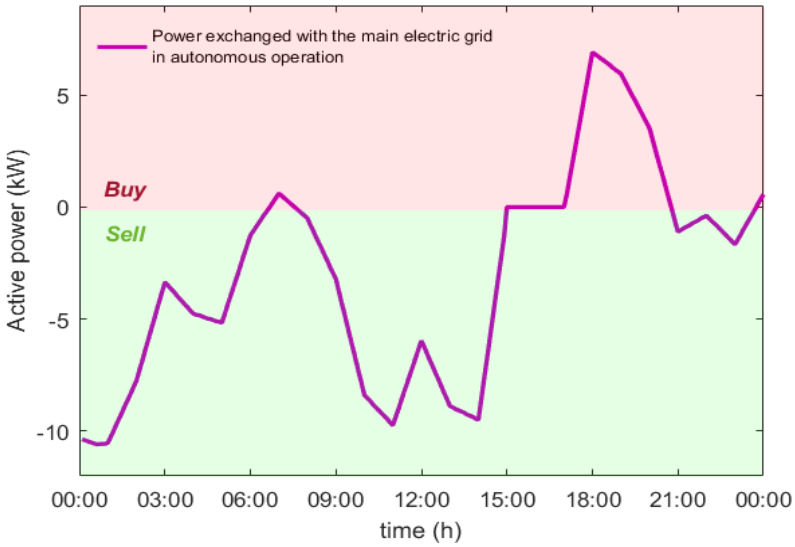

Fig. 31 Active Power Flow, Scenario II

Figure 32 shows the amount of energy stored in the battery during the day. As mentioned earlier, the battery stores energy during periods of low power demand and returns it when needed. Thus, during the first half of the day, when electrical loads are lower, a higher amount of stored energy is observed. Furthermore, the active power exchanged with the battery is shown in Figure 33. It illustrates the optimal use of the battery over a 24-hour period to minimize operating costs. Charging and discharging are indicated by plus and minus signs, respectively. Battery behavior during autonomous system operation, which occurs from 15:00 to 17:00, is also presented. Initially, a sudden drop in battery charge is observed due to grid disconnection. Around 16:00 p.m., the battery starts to get discharged as the electrical loads increase rapidly. However, even though the electrical load peaks in the next hour, the discharge rate is reduced at that time. This is because the system is connected back to the grid, which provides a percentage of the power needed. In any case, the battery plays an essential role in both grid-connected and autonomous operation of the system.

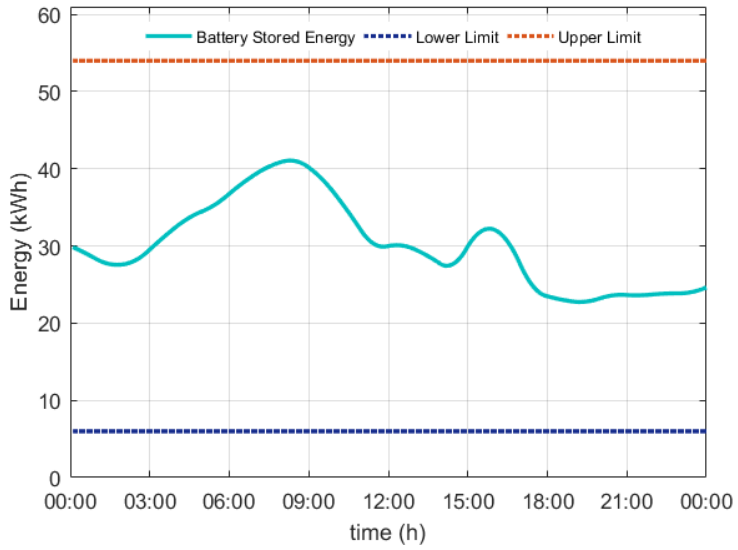

Fig. 32 State of Charge of the integrated Battery

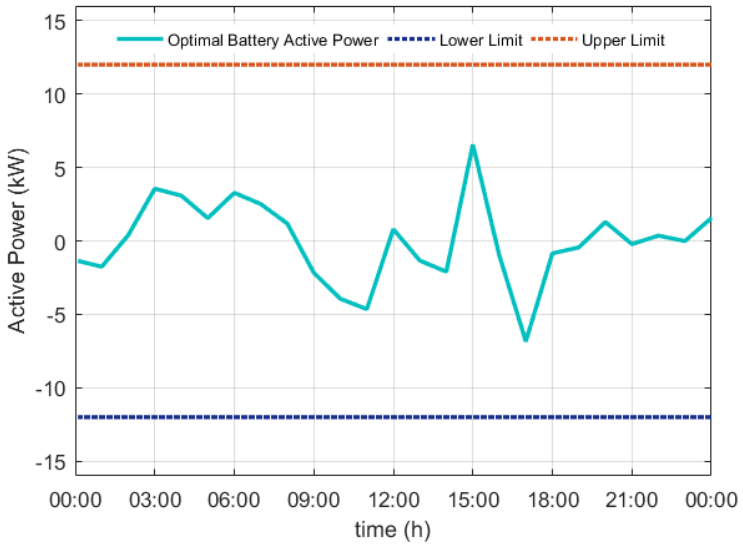

Fig. 33 Active power Exchanged with the Battery

In this scenario, the same operating strategy was applied as previously, i.e. “Following Thermal Load”. This results in a behavior similar to the scenario I. Thus, the majority of the thermal energy is provided to heat water during periods of low cooling demand. In this case, however, charging the battery during the night hours generates a greater amount of waste heat, as shown in Figure 34. This, in turn, is used to heat water since cooling demand is low during this period.

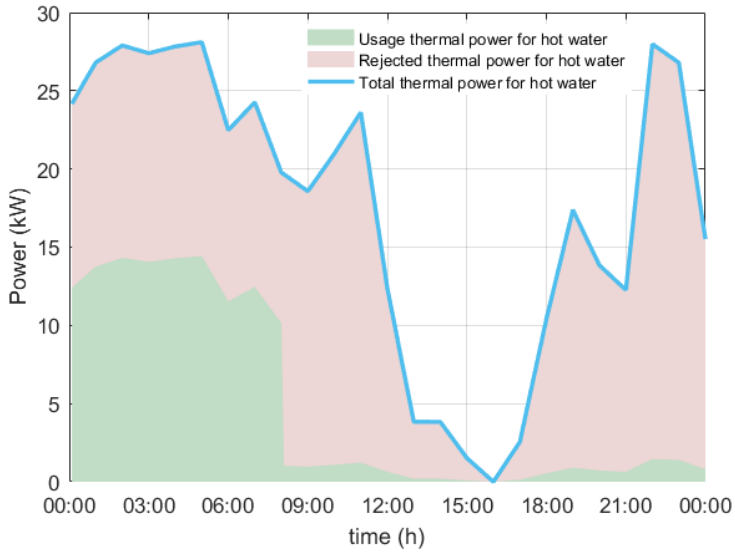

Fig. 34 Hot water thermal power, Scenario II

The fluctuations of the stored hot water during the 24-hour period are shown in Figure 35. During the night, cooling demand is low, and thus most of the waste heat is used to heat water. Meanwhile, hot water consumption is zero most of the time. Therefore, a steep increase in hot water storage is observed during this time. In comparison to the previous scenario, there has been an increase in the rate at which hot water is stored. This is due to the greater amount of waste heat generated during battery charging.

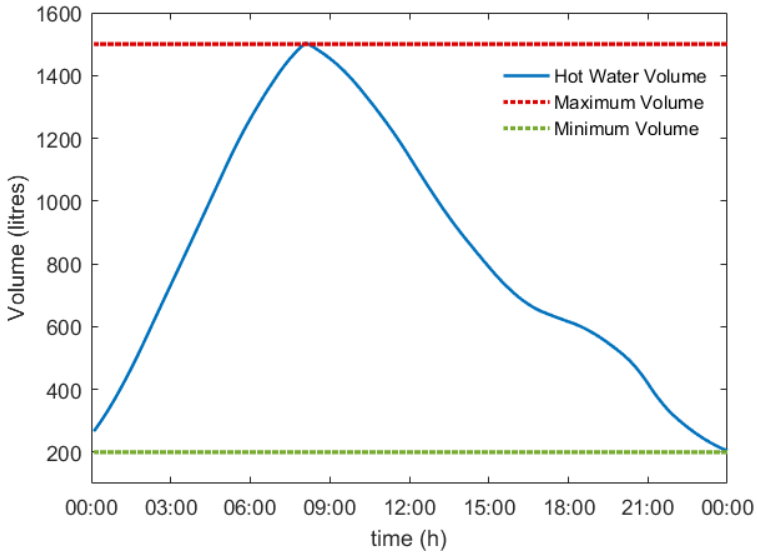

Fig. 35 Hot water volume in autonomous operation, Scenario II

PSO algorithm optimally schedules the CCHP system operation as shown in Figure 36. Since the operating strategy is the same for both scenarios, the uf factor has a similar behavior. Hence, it provides the thermal energy needed for cooling purposes. In this way, thermal zones temperatures are well maintained within the temperatures limits as presented above. However, higher CCHP system operating points are observed during the first half of the day. This is due to the battery charging process, which stores energy during periods of low demand. This can also be verified by the Figure 32, that shows the amount of energy stored.

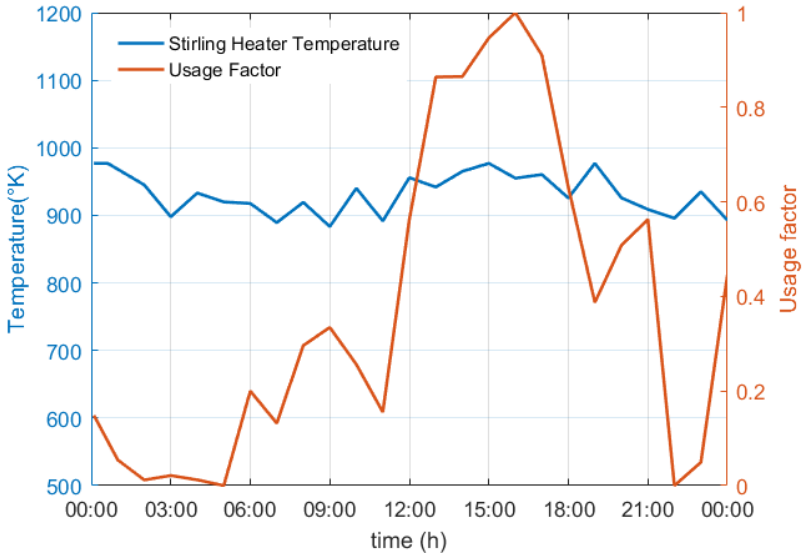

Fig. 36 PSO decision variable, Scenario II

In Scenario II, the total system operation cost is 7.9 $(m.u.)$. It is worth noting that both of the scenarios examined operate at nearly the same cost. Autonomous operation in Scenario II would have normally resulted in an increase in operating costs. However, the battery integration contributes to the optimal scheduling of the power exchange with the grid. In this way, it achieves a further reduction in cost throughout the day, which eliminates the additional cost of autonomous operation. As a result, operation costs for both scenarios are regulated in almost the same range.

Chapter 5

5. Conclusion – Future work

5.1 Conclusion

In this thesis, a CCHP system is proposed to provide the cooling, heating and electricity needs. Its operation is examined in applications corresponding to residential buildings. Furthermore, operational cost is optimized through the use of PSO algorithm over a 24-hour case study. A parametrized thermal model has also been developed for the prediction of representative thermal loads for a residential building. In this way, a variety of building structures can be studied simply by properly adjusting the parameters of the building being simulated. Flexibility indices are evaluated for each thermal zone of the building in terms of the zone temperature and defined lower and upper temperature limits. In this way, optimal distribution of thermal energy is achieved in all thermal zones according to the prevailing conditions. Electrical loads in Scenario I are powered either by the grid or by the system's generation unit. This selection, as observed in the results, depends on parameters such as grid electricity price during the day and aims to minimize the daily operating costs. In Scenario II, the system behavior is also investigated with the integration of a battery and an autonomous operation. Simulation results show the optimized scheduling with minimized operating costs for both scenarios. It is observed that despite the autonomous operation in Scenario II, the battery regulates the operating cost in the same range as in Scenario I.

5.2 Future work

There are several suggestions that could be adopted for future integration, which would help improve the current CCHP system and expand the scope of this thesis. In this way, the robustness and integrity of the system can be enhanced. However, those that are considered as the most important are presented below:

Electrical loads agent

Developing an Electrical Load model would benefit to control different types of the electrical loads of the building. More specifically, electrical loads can be classified into two types, critical and non-critical. Critical loads consist of devices, such as lighting, personal computers and TV’s, whose power consumption is specific and cannot be changed into different time slots . On the other hand, non-critical loads include devices, such as washing machines, that can flexibly shift their electricity consumption into different time slots during the day. This segregation of electrical loads allows non-critical loads to be shifted throughout the day to times of low electricity demand and low electricity price as well. As a result, further reduction of operating costs could be achieved.

Adjustable Thermal Loads

The use of real-time operation method of the Thermal Loads system would further improve system robustness. In more detail, some of the parameters of the models are difficult to be measured e.g. zone thermal gains, while others vary with time e.g. solar radiation, thermal conductivity of walls and windows. All of these parameters will be readjusted each time a change is observed. In this way, the method prevents deviations of proper system operation caused by uncertainties arising from the forecasted values.

Investigation under different building types

For further investigation of the system operation, a different type of building e.g. small commercial building, could also be modeled, as the characteristics and the energy needs differ depending on the use. Commercial buildings have a denser human presence and the human activity peaks at different time slots during the day. Additionally, thermal zones are spaced differently than in a residential building.

Integration into a microgrid

Microgrids constitute a developing area and are becoming more and more widespread. In addition, renewable energy sources have become a significant part of today's energy production. It is therefore well understood that distributed generation systems are going to be a fundamental change in the way that energy is produced. In this manner, it would be reasonable to examine trigeneration systems as a part of a microgrid since they are one of the most widespread distributed generation systems.

Renewable Energy Sources

The integration of the energy storage unit lays the groundwork for the use of renewable energy sources such as PV's. More specifically, apart from the main grid, PV’s will be an additional source of energy for the system. The energy produced by the PV's can either be stored in the battery or fed to the electrical loads. In this way, system autonomy is enhanced and operating costs can be further minimized. Therefore, RES integration may be another future extension of the current work.

References

[1] P.J Mago, L.M Chamra, J. Ramsay, "Micro-combined cooling, heating and power systems hybrid electric-thermal load following operation", Applied Thermal Engineering, vol.30, pp. 800-806, December 2009.

[2] L. Yaohong, T. Ran, W. Mingshan, " Operation strategy for interactive CCHP system based on energy complementary characteristics of diverse operation strategies", Applied Energy, vol.310, January 2022.

[3] X. Wang, Y. Xu, Z. Fu, J. Guo, Z. Bao, W. Li, Y. Zhu, "A dynamic interactive optimization model of CCHP system involving demand-side and supply-side impacts of climate change. Part II: Application to a hospital in Shanghai, China", Energy Conversion and Management, vol.252, December 2021.

[4] A. Asnaghi, S.M Ladjevardi, P. Saleh Izadkhast, A.H. Kashani, "Thermodynamics Performance Analysis of Solar Stirling Engines", May 2012.

[5] D.G. Thombare, S.K.Verma, "Technological development in the Stirling cycle engines", Renewable & sustainable energy reviews, vol. 12, pp. 1-38, July 2006.

[6] M. Sheykhi, M. Chahartaghi, M.M. Balakheli, B.A. Kharkeshi, S.M. Miri, "Energy, exergy, environmental, and economic modeling of combined cooling, heating and power system with Stirling engine and absorption chiller", Energy Conversion and Management, vol.180, pp.183-195, November 2018.

[7] N.A. Mpormpilas, June 2004, "Thermodynamic analysis of Stirling cycle", Doctoral Thesis, National Technical University of Athens.

[8] M. Chahartaghi, M. Sheykhi, "Energy, environmental and economic evaluations of a CCHP system driven by Stirling engine with helium and hydrogen as working gases", Energy, vol. 174, pp. 1251-1266, March 2019.

[9] M. Chahartaghi, M. Sheykhi, "Thermal modeling of a trigeneration system based on beta-type Stirling engine for reductions of fuel consumption and pollutant emission", Journal of Cleaner Production, vol. 205, pp. 145-162, September 2018.

[10] W. Martini, "Stirling engine design manual", NASA report, National Technical Information Services, US Department of Commerce, USA, April 1978.

[11] W. Martini, "Stirling engine design manual", NASA report, Second Edition, National Technical Information Services, US Department of Commerce, USA, January 1983.

[12] Arzu Sencan, Kemal A. Yakut, Soteris A. Kalogirou, "Exergy analysis of lithium bromide/water absorption systems", Renewable Energy, vol. 30, pp. 645-657, September 2004.

[13] G.A. Florides, S.A. Kalogirou, S.A Tassou, L.C. Wrobel, “Design and construction of a LiBr–water absorption machine”, Energy Conversion and Management, vol. 44, pp. 2483-2508, December 2002.

[14] S. Kalogirou, G. Florides, S. Tassou, L. Wrobel, “Design and Construction of a Lithium Bromide Water Absorption Refrigerator”, CLIMA 2000/Napoli 2001 World Congress – Napoli (I), 15-18 September 2001.

[15] Xiaohong Liao, Reinhard Radermacher, “Absorption chiller crystallization control strategies for integrated cooling heating and power systems”, International journal of refrigeration, vol. 30, pp. 904-911, January 2007.

[16] Syed Ihtsham-ul-Haq Gilani, Mojahid Sidahmed Mohammed Salih Ahmed, “Solution Crystallization Detection for double-effect LiBr-H2O steam absorption chiller”, Energy Procedia, vol. 75, pp. 1522-1528, March 2015.

[17] Holmgren, M. (2006), Mathworks, X Steam, Thermodynamic properties of water and steam.

[18] Meshram, A. (2013), Mathworks, Calculation of Enthalpy and LiBrH2O Concentration from curve-fitting equations.

[19] Kyriakou D.G., Kanellos F.D., “Optimal Operation of Microgrids Comprising Large Building Prosumers and Plug-in Electric Vehicles Integrated into Active Distribution Networks,” Energies, vol. 15, no. 17, pp. 6182, 2022.

[20] Jin X., Wu J., Mu Y., Wang M., Xu X. & Jia H., "Hierarchical microgrid energy management in an office building", Applied Energy, vol. 208, pp. 480-494, 2017.

[21] Kyriakou D.G., Kanellos F.D., “Sustainable Operation of Active Distribution Networks”, Applied Sciences, vol. 13, no. 5, p. 3115,2023.

[22] Estiri, H.; Zagheni, E. Age matters: Ageing and household energy demand in the United States. Energy Res. Soc. Sci. 2019, 55, 62–70.

[23] Csoknyai, T.; Legardeur, J.; Akle, A.A.; Horváth, M. Analysis of energy consumption profiles in residential buildings and impact assessment of a serious game on occupants’ behavior. Energy Build. 2019, 196, 1–20.